nature protocols

PROTOCOL

https://doi.org/10.1038/s41596-020-00489-8

Check for updates

Fabrication, characterization and applications of graphene electronic tattoos

Dmitry Kireev[1,2]✉, Shideh Kabiri Ameri[3], Alena Nederveld[1], Jameson Kampfe[1], Hongwoo Jang[4], Nanshu Lu[1,4,5,6] and Deji Akinwande[1,2,4]

Numerous fields of science and technology, including healthcare, robotics and bioelectronics, have begun to switch their research direction from developing 'high-end, high-cost' tools towards 'high-end, low-cost' solutions. Graphene electronic tattoos (GETs), whose fabrication protocol is discussed in this work, are ideal building blocks of future wearable technology due to their outstanding electromechanical properties. The GETs are composed of high-quality, large-scale graphene that is transferred onto tattoo paper, resulting in an electronic device that is applied onto skin like a temporary tattoo. Here, we provide a comprehensive GET fabrication protocol, starting from graphene growth and ending with integration onto human skin. The methodology presented is unique since it utilizes high-quality electronic-grade graphene, while the processing is done by using low-cost and off-the-shelf methods, such as a mechanical cutter plotter. The GETs can be either used in combination with advanced scientific equipment to perform precision experiments, or with low-cost electrophysiology boards, to conduct similar operations from home. In this protocol, we showcase how GETs can be applied onto the human body and how they can be used to obtain a variety of biopotentials, including electroencephalogram (brain waves), electrocardiogram (heart activity), electromyogram (muscle activity), as well as monitoring of body temperature and hydration. With graphene available from commercial sources, the whole protocol consumes ~3 h of labor and does not require highly trained personnel. The protocol described in this work can be readily replicated in simple laboratories, including high school facilities.

Introduction

Modern healthcare and biomedical systems show a clear trend towards personalized, predictive and preventive medicine[1]. The development of the concept commonly known as mobile health (mHealth)[2] means that a paradigm shift in medical device architectures is expected, thanks to the increased portability of medical devices as well as a rise in the number of smartphone apps[3,4]. One of the most significant problems in this field is the choice of functional elements and materials, since today's most common sensors are based on decades-old technologies. An ideal biomedical wearable device should possess the following set of essential requirements[5–8]: (i) The device must be mechanically intimately conformable to the skin. (ii) The device must be biocompatible. (iii) The technology must be multifunctional, i.e., allow measurement of various parameters at once. (iv) The fabrication protocol must be scalable and suitable for low-cost technology. The latter two criteria are of particular importance when it comes to the development of point-of-care wearable biomedical patches that can be applied to the skin for physiological measurements[9]. Such patches could be made with off-the-shelf (OTS) components and promptly available to the end-users: individuals who can apply it on themselves at their demand or convenience. When connected to a readout device (e.g., a phone or tablet), the patch must be able to detect a plurality of vital signals (e.g., heart rate, hydration, temperature, brain waves).

Regardless of the massive value of the global wearable technology market (>US$74 billion by 2025)[10], the majority of modern gadgets are surprisingly stiff, rigid and bulky. In the best contemporary examples, there is a flexible and soft shell (ribbon or sticky patch), while the primary sensor and electronics are rigid[5,11–13]. The connection is hindered by the silicon technology itself, which cannot readily offer a facile solution due to the mechanical mismatch between stiff and hard

[1]Department of Electrical and Computer Engineering, The University of Texas at Austin, Austin, TX, USA. [2]Microelectronics Research Center, The University of Texas at Austin, Austin, TX, USA. [3]Department of Electrical and Computer Engineering, Queen's University, Kingston, Ontario, Canada. [4]Texas Materials Institute, The University of Texas at Austin, Austin, TX, USA. [5]Department of Biomedical Engineering, The University of Texas at Austin, Austin, TX, USA. [6]Department of Aerospace Engineering and Engineering Mechanics, The University of Texas at Austin, Austin, TX, USA. ✉e-mail: kirdmitry@gmail.com

materials (silicon, glass, metals, high-κ dielectrics), and the tissue, which is soft, squishy and stretchable.

The development of such wearable and low-cost ultrasensitive devices is essential in the view of the recently established progressive mHealth concept[2], which converges on so-called 4P medicine[1]: personalized, preventive, predictive and participatory. In this regard, the sensors and devices must be wearable, i.e., be in close contact with the human skin, and be able to measure and transmit biomedical, electrophysiological or chemical data without influencing the body's regular operation. Yet, they should be simple enough for the subjects to administer them unassisted.

Two-dimensional (2D) materials are unique forms of more conventional materials. When the same atoms are arranged into a single plane, i.e., confined strictly to a one-atom-thick conformation, the materials start to exhibit novel properties[14–17]. Graphene, in particular, possesses tremendous potential for the development of next-generation, wearable and soft biosensors[18,19]. Several graphene-based devices, such as graphene field-effect transistors[20], graphene-based microelectrodes[21] and graphene electronic tattoos (GETs)[22–24] have recently been developed. They are used for a large variety of healthcare applications, such as cell electrophysiology, biosensing and environmental monitoring[18,25,26]. The most important features of graphene, however, are its intrinsic flexibility, transparency and softness[27,28]. The advanced properties of graphene have enabled the extraordinary opportunity to substitute standard silicon and rigid metal films with the ultimately flexible material[29]. Graphene's outstanding performance is associated with its sub-nanometer thickness, allowing it to bend, flex and stretch while retaining much of its intrinsic properties. Graphene-based electronic tattoos are ideal candidates for a variety of mHealth applications, including recordings of electrophysiological and physiological data[22,26]. It is essential to mention that GETs are atomically thin, optically transparent and mechanically imperceptible. Due to GETs' ultrathinness, they are perfectly conformal to the micro-curvature of skin; therefore, they are much less susceptible to motion artifacts. Furthermore, graphene tattoos allow for the normal function of the human skin during measurements, unlike the standard gold-, silver- or gel-based electrodes, which are not transparent and block access to the surface of the skin by visible and ultraviolet light. In this protocol, we provide step-by-step procedures for the fabrication and characterization of GETs as well as a selection of biomedical application examples.

Development of the protocol

We first reported the usage of graphene for epidermal electronics and healthcare monitoring in 2017[22]. In the inaugural work, GETs were successfully used for epidermal monitoring of heart activity (electrocardiogram (ECG)), muscle activity (electromyogram (EMG)), brain waves (electroencephalogram (EEG)), skin temperature and skin hydration (see Figs. 1, 2). Historically, the method described in the work is a partial adaptation from the 'cut-and-paste' process[30–33] developed earlier by Lu and coworkers. The 'cut-and-paste' method utilizes a benchtop OTS cutting tool to mechanically carve out the required patterns of thin conducting and metal-covered thin films on the scale of ≤12 inches wide and several feet long. Typically, the carved patterns are supported by thermal release tapes (TRTs) whose adhesiveness is later reversed, freely suspending the final structures. However, the original 'cut-and-paste' method[31] utilizes certain steps, such as TRT support, that we found to be incompatible with graphene, motivating an adapted protocol specifically for graphene. Before developing the protocol as reported here, we searched and experimented with multiple methodologies to achieve a straightforward technique that results in reasonable quality and yield. Following copious trials of various recipes, including attempts to find a suitable handling polymer (including polyimide and other spin-coatable polymers), and attempts to modify the transfer and handling procedures, a working procedure was eventually developed and reported in the inaugural work[22]. The current method features usage of poly(methyl methacrylate) (PMMA) as graphene's support polymer and temporary tattoo paper as the transient substrate with hybrid nature (see the Procedure details, Steps 10–12). When dry, the temporary tattoo paper adheres well to the graphene during manufacturing, yet it can release graphene from its surface when wet to facilitate transfer onto the skin. Taking advantage of this intimate contact with the skin and graphene's optical transparency, we placed GETs onto the human face to build an interface to a machine. By placing the GETs above, below and to the side of the eyes, it was straightforward to distinguish and monitor the eyeballs' movements in real-time. The signal is then processed online in real time and sent directly to a drone (see Fig. 3) that flies according to the subject's direction of sight[23]. In subsequent research, we have significantly refined the protocol, as shown in detail in this document, resulting in higher device

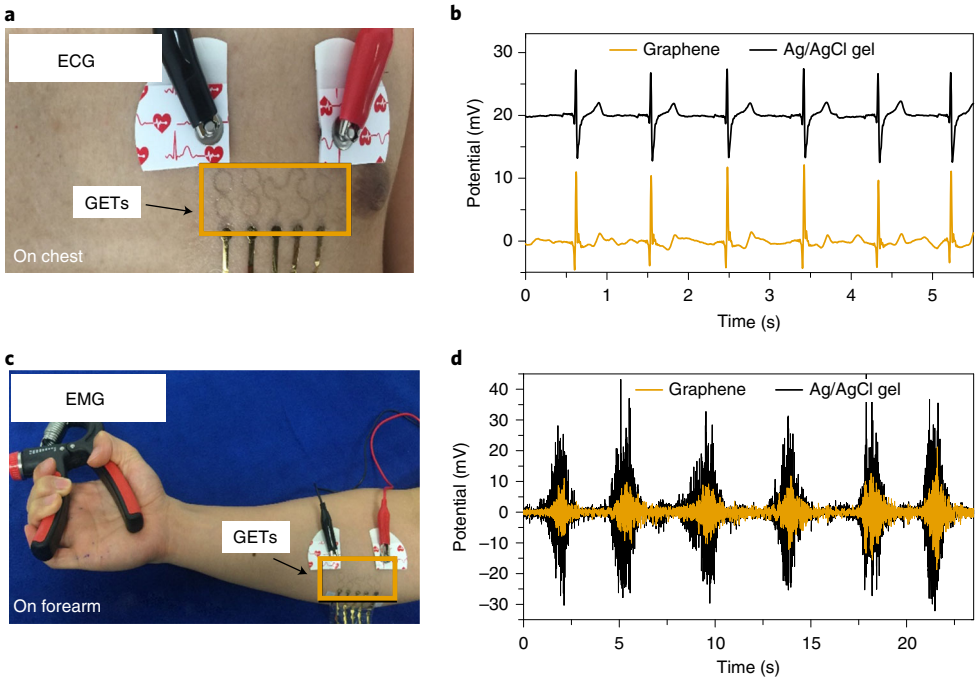

Fig. 1 | Use of GETs for electrophysiological sensing. a,**b**, Image of graphene array transferred onto a human chest and used for standard ECG monitoring, with results shown in (**b**). **c**,**d**, The graphene array transferred onto a human forearm and used for muscle activity (EMG) monitoring (**d**). In both (**b**) and (**d**) the data from graphene is shown in dark yellow, and commercial Ag/AgCl gel electrodes in black for direct comparison. The black and red wires in **a** and **c** represent electrical cables required for electrophysiological recordings from Ag/AgCl gel electrodes. Adapted with permission from ref. [22], American Chemical Society.

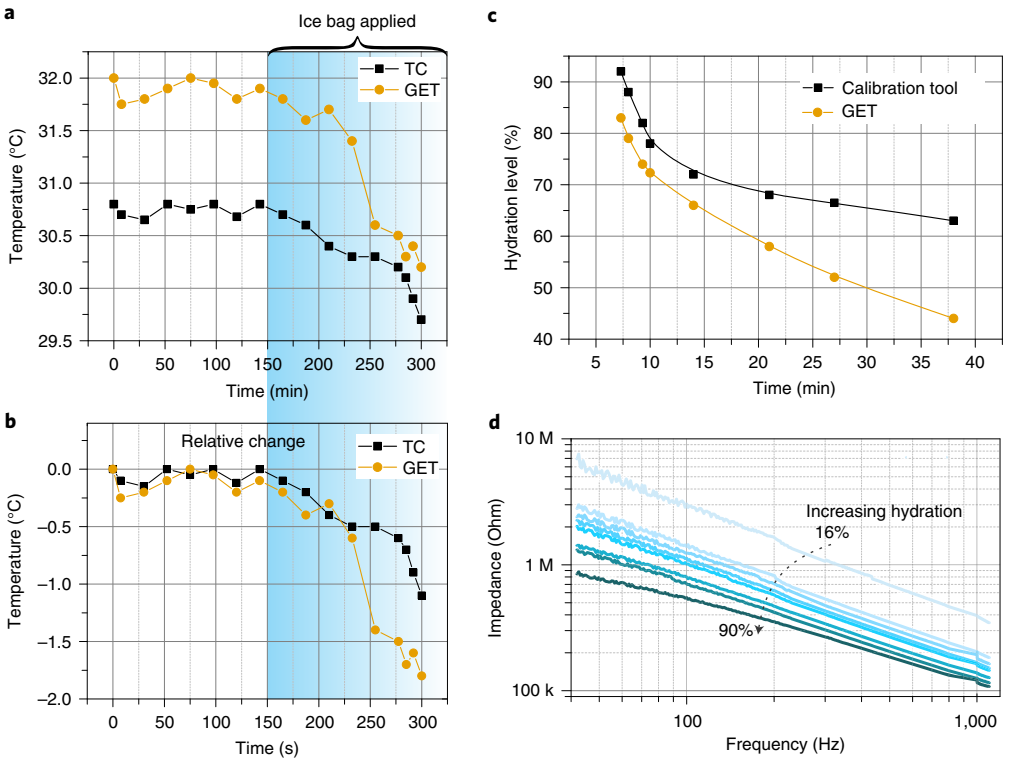

Fig. 2 | Monitoring skin temperature and hydration via GETs. The absolute (**a**) and relative (**b**) change of temperature recorded by a thermocouple (TC) and a GET upon application of an ice pack on top of the array. **c**, The timetrace of human skin's change of impedance monitored with both an industrial calibrated tool and a set of GETs upon drying of the skin over time. **d**, Detailed impedance characterization of the GETs while skin hydration changes from 16 to 90%. Adapted with permission from ref. [22], American Chemical Society.

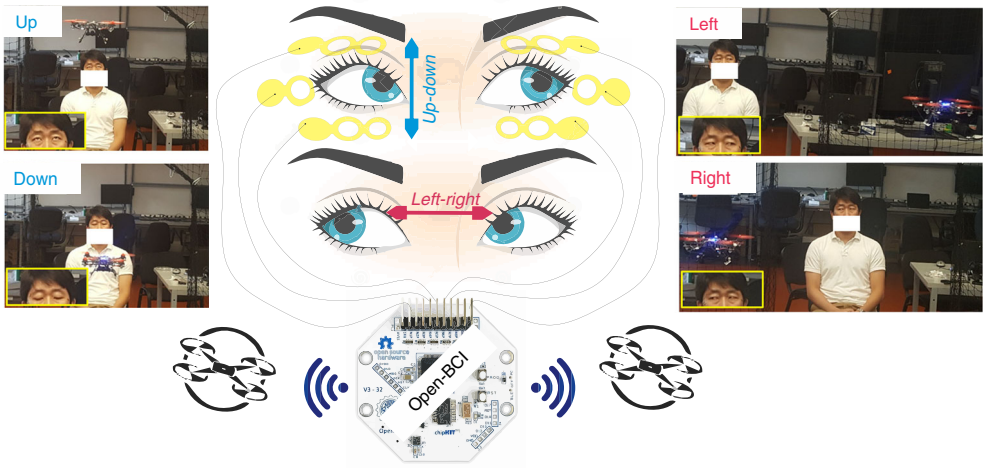

Fig. 3 | Schematics of GET-based electrooculography and its use for HMI. A set of GETs (yellow) placed above, below and to the sides of human eyes are used to record EOG signals that are acquired via an open-source platform, processed online and sent directly via Bluetooth to a nearby quadcopter (black). The quadcopter flies according to the specific patterns of eye movements. Adapted from ref. [23], Springer Nature.

quality and increased yield, and featuring a more optimized way to provide electrical contacts to the graphene. A significant improvement in the electrical properties of the GETs has been achieved by establishing double and triple graphene layer structures by multistacking monolayer graphene (see Box 2 for details). The multistacked few-layer GETs feature lower sheet resistance while retaining much of the mechanical and optical qualities of monolayer GETs. When using a monolayer graphene tattoo, wrinkles and cracks (caused by the chemically vapor-deposited (CVD) growth or the transfer) result in a huge deviation of the electrical properties. As can be seen from the Anticipated results section, most of the monolayer samples have a large standard deviation of their parameters, mainly due to the above-mentioned imperfections. Using multilayer graphene structures provides much more reliable electrical pathways, and even if a single graphene monolayer has certain defects, they are circumvented due to the presence of the second graphene monolayer in direct contact. Most recently, we have used these few-layer GETs to observe tissue bio-impedance with the scope of moving towards continuous blood pressure monitoring[24].

It is important to emphasize that this protocol leverages CVD graphene, a high-quality and large-area material[34], allowing us to develop low-cost, wearable and entirely conformal skin patches that are scalable. The fact that these devices can be efficiently fabricated via inexpensive, easily available OTS tools makes the technology valuable for future industrial implementation.

Overview of the procedure

The procedure described here consists of seven main stages, divided into 27 steps. In Steps 1–4 we discuss how to perform CVD growth of graphene; these steps can be replaced by using commercially available CVD-grown graphene on copper foil. Upon growth or purchase of the graphene, its quality should be evaluated. The most common and nondestructive method for the evaluation is Raman spectroscopy (Step 5). Box 1 shows examples of Raman spectra of monolayer graphene with different qualities. We then describe the necessary steps of preparation of the graphene/copper foil (Steps 6–9) and temporary tattoo paper (Steps 10–12) for the transfer. Repeating Steps 6–9 twice results in the creation of a multilayer graphene stack and, consequently, bilayer graphene tattoos (bi-GET), which were shown to have advanced electrical properties compared to monolayer GETs. Box 2 explains the procedure of bilayer GET creation. The process of transfer of the graphene from copper foil onto temporary tattoo support is described in full detail in Steps 13–19, with Supplementary Video 1 provided for visual guidance. After graphene is fixed on a tattoo paper, it is carved into a specific pattern via a mechanical cutter machine, as explained in Steps 20–23 and two Supplementary Videos provided for visual aid. Simply placing GETs onto skin is not enough, and a soft yet robust and stretchable electrical contact to harder electronics is required for fault-free operation. Hence, we developed conductive, ultrathin, soft and adhesive tape, which is used as the essential intermediary

Box 1 | Monolayer graphene quality check via noninvasive Raman imaging

Raman is an immensely valuable tool that can be used to study graphene properties, including doping level, electron–phonon interaction, the density of defects, etc. Generally, it is possible to evaluate and estimate the quality of graphene via a quick look at its Raman spectrum. The main Raman responses in graphene are the primary in-plane vibrational mode **G peak** (1,580 cm^{-1}) and the **2D peak** (2,690 cm^{-1}), which is the result of a two phonon lattice vibrational process. Another notable peak is **D peak** (1,350 cm^{-1}), a disorder peak, corresponding to a breaking peak of an sp^2 ring close to an edge or a defect[76]. The widths and locations of the peaks correspond to layer number and level of doping. The most common and easy to perceive figure of merit, however, is the ratio of 2D peak intensity over G peak intensity, I_{2D}:I_G. The larger the proportion, the higher quality, better graphene. Conversely, when the I_{2D}:I_G ratio is equal to or less than unity, the graphene is of rather low quality.

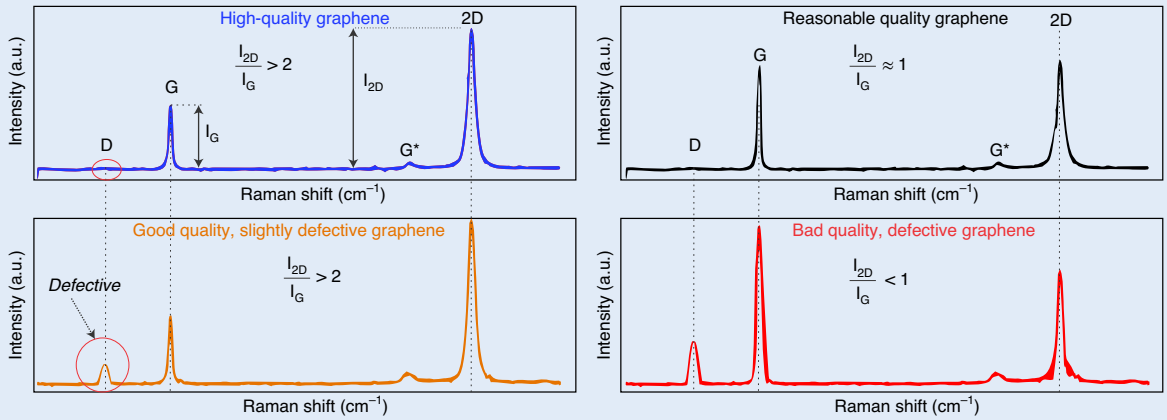

In the case of GETs, however, it is close to impossible to perform Raman spectroscopy on the final device due to the presence of the PMMA support layer. PMMA, along with most of the organic polymers, introduces a sizeable fluorescent background, hindering the Raman fingerprints of graphene. Therefore, the Raman study is usually performed on the copper foil before transfer, or on the graphene transferred onto a dummy SiO_2/Si wafer.

and contacts graphene on one side and harder electronics on the other. The details of soft adhesive conductive tape fabrication are given in Box 3, and the complete routines for establishing the contacts to graphene via copper tape or silver epoxy are given in two options of Step 24. Supplementary Videos are provided for accurate guidance. In Step 25, we describe the most essential yet challenging part of the procedure: transfer of the GET from paper onto skin. This stage is supplemented with comprehensive visual assistance via Supplementary Video 6. In four sections of Step 27, we describe how the graphene tattoos (already placed on skin) can be used for skin impedance checks (Option A), skin hydration monitoring (Option B), temperature monitoring (Option C) and low-cost monitoring of EEGs, EMGs or ECGs (Option D).

Applications

As briefly discussed in 'Development of the protocol', the GETs can be successfully used towards the continuous monitoring of multiple physiologically important biomarkers. If upscaled and used habitually, GET technology can be of help to doctors, clinicians and researchers in understanding and perhaps finding treatments for certain diseases. For example, to robustly record a subject's heart rhythms (ECGs), as few as two GETs placed on a chest (see Fig. 1a,b) or on two arms is sufficient. This application alone opens up a distinct technological advance, allowing the development of a simple tattoo-style patch that is intimately wearable and comfortable, yet provides continuous ECG monitoring on par with the state-of-the-art Holter monitors[35]. Furthermore, human body temperature must be kept within a small range to be healthy. GETs have been reported to provide a remarkably high sensitivity to skin temperature variations, as can be seen from Fig. 2a,b. The GET's temperature response is on par with the performance of a classic thermocouple. Likewise, skin hydration (Fig. 2c,d) can be monitored explicitly by the same GETs, allowing for an advanced lightweight yet robust and wearable sensor that can be useful for diverse applications, including multi-function and lightweight use cases[36,37].

Muscle-activity monitoring, EMG, is another application where GETs can find widespread use. Recording a specific muscle's electrical activity takes two GETs biased in a differential mode. The prominent advantages of graphene in comparison to other standard electrodes are their size and

Box 2 | Creating few-layer graphene ● Timing 30 min + 12 h

We have found experimentally that bilayer graphene electronic tattoos (biGETs) feature higher stability, better electrical properties, and superior contact impedance. This superiority can be partially attributed to the formation of so-called graphene nanoscrolls during the etching of the copper foil. The reason behind this is that during CVD growth, graphene also grows on the back side of the copper foil (usually of lower quality). If not explicitly removed, then the back-side graphene rolls into itself during the copper etching and creates the so-called nanoscrolls[77].

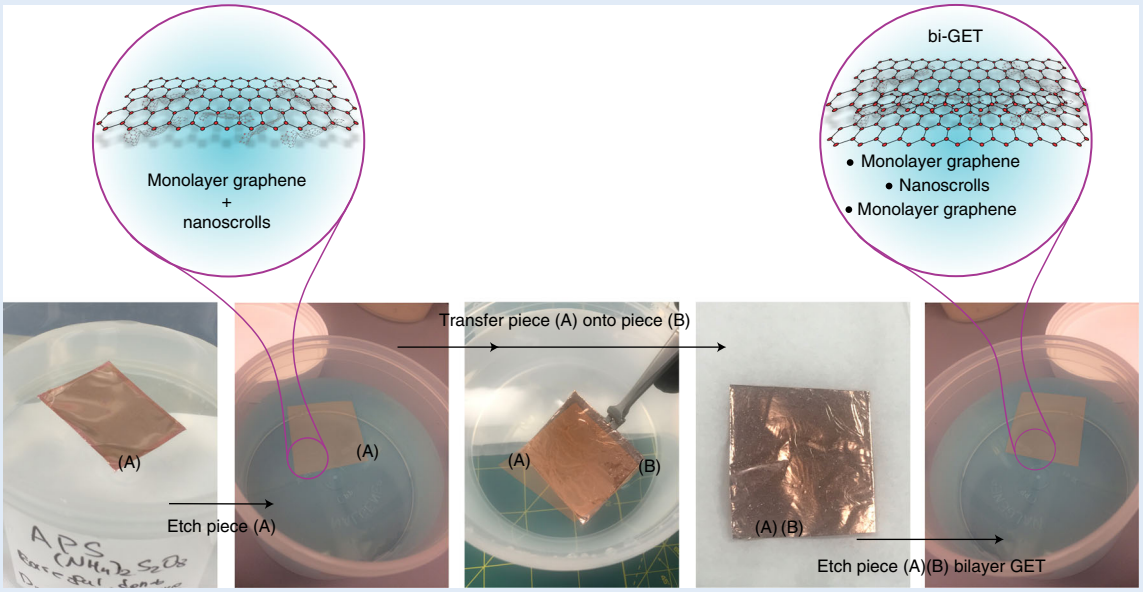

Procedure

1 Prepare one piece of PMMA/graphene/copper (A) accordingly to Steps 6–9, and place it into copper etch, as described in Step 13.
2 When the etching is complete, transfer into clean DI water according to Steps 14–15.
3 Prepare another piece (B) of graphene/copper, this time bare, without PMMA.
4 Use piece (B) to fish out piece (A).
5 Carefully place the stack on a tissue and leave to dry slowly at room temperature (~25 °C) overnight.
6 Anneal the (A)-(B) stack at 200 °C for 10 min to reflow the PMMA and establish a good adhesion.
7 Etch copper again, and continue with Step 13 onwards.

The resulting bilayer (A)-(B) stack is what we call **bi-GET**. It is, however, morphologically and electronically different from directly CVD-grown bilayer graphene that has an extra interlayer stacking. Moreover, it is possible to avoid the formation of nanoscrolls if the back side of the copper foil is exposed to an oxygen plasma that etches away the graphene before the copper etch. In this case there will be no nanoscroll formation, if this is required.

ability to be precisely located without any further misplacement during operation. It allows intimate contact and provides the capability to record from a specific muscle that is essential for building next-generation human-machine interfaces (HMIs). As can be seen from Fig. 1c, a pair of GETs on a forearm is compared alongside the standard Ag/AgCl gel electrodes. Despite graphene's tenfold smaller size and electrode spacing, we recorded highly useful EMG signals that can be used to build comfortable HMIs[23,38]. Similar to EMG, there is a so-called electrooculography (EOG). EOG signals are biopotentials associated with the eyeballs' movements. Technically, EOG electrical potentials are the results of hyperpolarizations and depolarizations between the cornea and the retina[39]. In order to measure EOG signals, GETs are placed above, below and to the sides of the eyes. As shown in Fig. 3, GETs afford very accurate eyeball tracking. The recorded EOG information (subject looking up, down, left, or right) can be further processed online and sent to a quadcopter that flies according to the eyeballs movements[23]. Moreover, the transparency of the GETs affords enhanced visual aesthetics, which is not possible with standard gold or Ag/AgCl gel electrodes.

As presented in our most recent work, the same GETs can be used not only for passive biopotential recordings but also for active electrical human biopotential recordings, namely tissue bioimpedance[24]. This can be done by placing ≥4 GETs in a row, using the two outer electrodes to inject an AC current (within allowed amplitude range), and using the inner two GETs to record the corresponding AC voltage change. This four-probe technique allows direct measurement of the tissue

Box 3 | Preparation of ultrathin conductive feedlines ● Timing 3 h

Procedure

1 Take a roll of Kapton tape or any other ultrathin tape. Ideally, the thickness must be much less than 1 mil (<25 μm). A commercially available ultrathin adhesive polymer film (Iwatani, ISR-BSMK10G) that we found to serve the purpose successfully has a thickness of ~10 μm and a sticky backing layer that provides adhesion to the skin.
2 Evaporate a layer of conductive metal on top, e.g., 10 nm Ni followed by 90 nm of Au. Make sure the temperature does not rise too high (<60 °C) to ensure the physical integrity of the thin films and adhesives.
3 Cut the conductive adhesive tape into strips of required length.

impedance (mΩ) bypassing the significantly larger skin impedance (kΩ). The impedance can then be monitored for a very long time. Depending on GET placement, one can aim towards monitoring blood flow hemodynamics, respiration rate or perhaps inner organ functions[24,40,41].

In a much broader view, GETs have already been used in combination with other techniques conventional in the fields of healthcare and bioelectronics, i.e., for in vivo electrophysiology[42], UV exposure monitoring[43], pressure sensing[44], the development of electronic skin[45,46] or next-generation prosthetics[47]. Moreover, the tattoo integration process can be adapted for other 2D materials, enabling the vision of fully 2D wearable electronics[18,48].

Limitations

There are a few limitations of the GET technology. The unambiguously good adhesion and imperceptible contact to the skin are associated with the soft characteristics of graphene. While GETs sustain ≤30% strain on the skin[22], the devices are nonetheless vulnerable to scribing, scratching or excessive shear pressure. It is a crucial future engineering task to enable tougher yet wearable protection/enclosure to the GETs that will not affect tattoo performance. Establishing interconnection to GETs is another essential problem to solve. GETs are only 200 nm thick, but they must be connected to a back-end-circuit via much thicker and stiffer electrical connectors. The weakest point (fracture point) under deformation will be the interconnection due to the stiffness mismatch. Although GETs are stretchable enough to survive normal on-skin conditions, the overall stretchability (GET + back-end-circuit) still needs to be improved to develop fully integrated graphene-based wearables[49–51]. Within this protocol, we demonstrate two examples of establishing intimate electrical contacts to graphene tattoos. We utilize the thinnest possible market-available sticky tape with evaporated conductive layer of gold on top of it. This ultrathin conductive gold tape serves as the intermediary interconnection. It is soft enough to provide mechanical coupling with the graphene tattoo. The other side of the soft gold tape is then coupled to a stiffer copper tape (Step 24, Option A) or directly soldered via silver epoxy (Step 24, Option B).

Another challenge with GETs is the choice of graphene source. While the technology has improved over the last decade, the quality of large-scale CVD graphene still varies from supplier to supplier. Besides, regardless of supplier, the use of single monolayer graphene is challenging. As shown in the Anticipated results section, monolayer graphene-based tattoos performance varies significantly, which can be attributed to (i) the presence of grain boundaries that limit charge transport; and (ii) the existence of micro and macro cracks in the cm-scale samples. To overcome this limitation, we propose using multi-stacked few-layer graphene tattoos (see Box 2 for details on multilayer GET fabrication) that show superior performance and stability.

Comparison with other methods

Wearable electronic tattoo sensors, placed directly on the skin, have recently gained importance, especially for point-of-care and low-cost personalized medicine[52,53]. These sensors can be used outside of hospital settings, allowing for broad applications such as mHealth and remote monitoring of vital signals. The technologies presently used for electrophysiological measurements either are based on bulky point-contact electrodes that are placed onto the surface or subsurface of the skin[54,55] or utilize conducting gel. For example, the most common EEG hardware consists of gold cups that are firmly fastened onto the skull and filled with a conducting gel electrolyte. For many applications, the skin is also prepared explicitly by abrasion to reduce the contact impedance, a procedure that is time-consuming, uncomfortable and unsuitable for long-term recordings since the conductive gel dries out with time.

There are two main approaches currently under extensive research and development, which are used by scientists and engineers to build skin-conformable wearable electronic devices. One approach has its roots in the advancements of general materials science and engineering. It is based on the utilization of recently discovered novel materials, such as ultrathin and soft electrically conductive polymers, semiconducting nanotubes[56], nanowires[57], dielectric fibers or their mixtures[57]. Numerous soft, flexible and electrically functional polymers have been recently discovered or chemically engineered[58–62]. Polyanilin[62], chitosan[62] and PEDOT:PSS[63,64] are just some of the common functional and mixed polymers that have been recently used. Embedding these soft polymers onto the skin is a much easier method and very similar to the approach that is employed in graphene tattoo technology. Since the devices are soft, they feature advanced adhesion to the skin, increased comfort and more intimate interface, and, therefore, increased sensitivity of electrophysiological recordings.

The other approach is based on creating filamentary serpentine structures from bulky and generally rigid and non-stretchable materials (e.g., gold or silicon)[12,65–67]. The method was first developed by Rogers and co-workers and called 'epidermal electronics'[12]. It enables a drastic reduction in the stiffness of conventional electronic systems without appreciable loss in their electronic functionality, while at the same time increasing the flexibility and capacity to laminate these devices onto the skin. This approach's main feature is embedding small islands of stiff and rigid devices into a bed of soft and flexible polymer. Such a hybrid approach is utilized in the majority of commercially available epidermal and implantable biosensors for numerous applications[5,67].

To date, epidermal sensors have been successfully used to monitor EEG[68], ECG[59], EMG[12], EOG[23], skin temperature[69], skin hydration level[66], sweat[70], pH[71], and more. Nonetheless, a long-term and non-irritating coupling to the skin is one of the main challenges of the classic wearable device. In this regard, the ultrathin profile of graphene and 2D materials makes them ideal candidates for applications due to their conformability to uneven and irregular yet stretchable surfaces, such as skin[28]. GETs exhibit strong adhesion to the skin via the van der Waals force and no additional adhesive or encapsulation layer is required for the attachment.

Comparing the GETs discussed in this work to the alternative approaches mentioned above shows that the main advantage of graphene over all other methods is complete optical transparency (>85%), which is not the case with polymer- or gold-based systems. The electrical performance of GETs is somewhat smaller compared to that of medical grade gel electrodes, but the same is true for all other epidermal and tattoo sensors (see Supplementary Table 1 for detailed comparisons). Another clear distinction of GETs is their excellent adhesion to skin, which is self-adherent, with only a handful of other works featuring ultrathin gold nanomesh electrodes that report the same efficiency[72,73]. In contrast, the majority of the previously reported edipermal electronic sensors and tattoo sensors still require some sort of adhesion or support[32,68,74].

Another alternative to the ultraconformable graphene tattoos described in this work are graphene flexible sensors, such when graphene is placed onto thicker (25–100 μm) polyimide support[22]. Such devices can also be used for electrophysiological sensing, but they do not form intimate contact with the skin, are much thicker and not entirely transparent (due to the polymer substrate). Alternative methods for GET fabrication could perhaps be utilized, such as laser-assisted instead of mechanical cutting[75]. Graphene itself could also be pre-shaped by using oxygen plasma cleaning, maybe even before transferring from the copper foil. Such modifications, however, would only increase the complexity of the overall method. The protocol as described here is a downscaled method that yields excellent GET quality while using the simplest tools possible. Moreover, we believe that the proposed protocol has the capacity to be automatized, upscaled and industrialized in the future.

Materials

Reagents

- Copper foil (Alfa Aesar, cat. no. 10954)
- Methane (CH_4; Airgas, cat. no. ME R300DS)
- Hydrogen (H_2; Airgas, cat. no. HY R300)
- Ammonium persulfate ($(HN_4)_2S_2O_8$) for copper foil etch (Sigma-Aldrich, cat. no. 248614) **! CAUTION** Ammonium persulfate is harmful if swallowed and can cause skin irritation and eye damage. Wear gloves and safety glasses when handling.
- Nitric acid (HNO_3; Sigma-Aldrich, cat. no. 438073) **! CAUTION** Nitric acid is harmful if swallowed and can cause skin irritation and eye damage. Wear gloves and safety glasses when handling.
- Ultrapure deionized (DI) water (18.2 MΩ·cm; Millipore, Milli-Q system)

- PMMA (950 PMMA A4; MicroChem Corp., cat. no. M230004) **! CAUTION** PMMA is a highly flammable liquid. Keep it away from heat and static discharge. While handling, wear proper eye and face protection.
- Silver Epoxy Adhesive (MG Chemicals, cat. no. 8331S)
- Monolayer CVD-grown graphene: this can be prepared according to Steps 1–4 of the Procedure or ordered from commercial sources, e.g., Graphene Supermarket (https://graphene-supermarket.com/Single-Layer-Graphene-on-Copper-foil-4-x4-CVD-Cu.html), Graphenea (https://www.graphenea.com/collections/buy-graphene-films/products/monolayer-graphene-on-cu-with-pmma-coating-4-inches) or Grolltex (https://grolltex.com/product/monolayer-graphene-on-copper-foil-6-x-6-150-mm-x-150-mm/) **▲ CRITICAL** The worldwide market for graphene materials has been expanding drastically, and the increasing demand for high-quality monolayer graphene has been increasing the supply and driving the costs down. In Supplementary Table 2, we provide the comparative costs of the current (October 2020) market prices for monolayer graphene. The lowest cost of graphene now is US $0.5/cm^2. However, even these prices are expected to be reduced by an order of magnitude in the next few years, when the higher product demand will force tcompanies to scale up their fabrication.

Equipment

- Silicon (Si) wafers (NOVA, cat. no. HS39626-WO)
- Tweezers (e.g., VWR, cat. no. 102098-992)
- Hot plate (Four E's Scientific, cat. no. MI0102003V11-POI)
- Acid chemical hood (e.g., Fisher American, cat. no. NLS-420)
- Lab scales (Escali, cat. no. L125)
- Mechanical cutter (Silhouette cameo, 3 https://www.silhouetteamerica.com/shop/cameo/SILHOUETTE-CAMEO-3-4T)
- Auto blade (Silhouette America, https://www.silhouetteamerica.com/shop/blades-and-mats/SILH-BLADE-AUTO)
- Cameo cutting mat—light adhesion (Silhouette America, https://www.silhouetteamerica.com/shop/CUT-MAT-12LT)
- E-beam assisted metal evaporation tool (e.g., CHA Industries, SEC-600/SE-600)
- Raman spectrometer (e.g., Renishaw inVia)
- Open electrophysiology board (e.g., OpenBCI, Ganglion board, https://shop.openbci.com);
- Handheld LCR meter (Keysight Technologies, cat. no. U1732C)
- General-purpose LCR meter (e.g., Hioki IM3536)
- (Optional) Skin hydration meter (e.g., Delfin Technologies, MoistureMeterSC)
- (Optional) B2902A precision source/measure unit (e.g., Keysight, cat. no. B2902A)
- (Optional) Thermocouple and temperature reader (e.g., Amprobe, cat. no. TMD-56)
- (Optional) CVD system for graphene growth (e.g., Black Magic, Aixtron)
- (Optional) Reactive ion etch or oxygen plasma tool (e.g., Plasma-Therm, cat. no. RIE 790)
- Wipes (VWR, cat. no. 21905-049)
- Petri dishes (Sigma Aldrich, cat. no. BR452005)
- Wide beakers (Nalgene cat. no. 2118; Sigma Aldrich, cat. no. Z380253)
- Razor blades (e.g., OEM Tools, cat. no. 25181)
- PI-based sticky tape (e.g., VWR, cat. no. 89495-448)
- Tattoo paper (https://www.amazon.com/Silhouette-MEDIA-TATTOO-Temporary-Tattoo-Paper/dp/B0043WJ3OA) **▲ CRITICAL** Different tattoo papers utilize different layer structures. Some of them might be incompatible with the protocol described here.
- Ultrathin adhesive polymer film (Iwatani, cat. no. ISR-BSMK10G)
- Conductive copper tape (Oubaka, cat. no. HQGOODS-002) **▲ CRITICAL** Copper tape provides essential strong yet soft support to skin, and supports the metal to be evaporated on top.
- Kind removal silicone tape (KRST; 3M, cat. no. 2270-2)
- Tegaderm (3M, cat. no. 1624W)
- Surface Ag/AgCl gel electrodes (Bio-Medical, cat. no. H135SG)
- (Optional) Liquid bandage (3M Nexcare, cat. no. 118-03)

Software

- Keysight GUI Data Logger Software For Handheld LCR Meter (https://www.keysight.com/main/software.jspx?ckey=1953070&cc=US&lc=en)

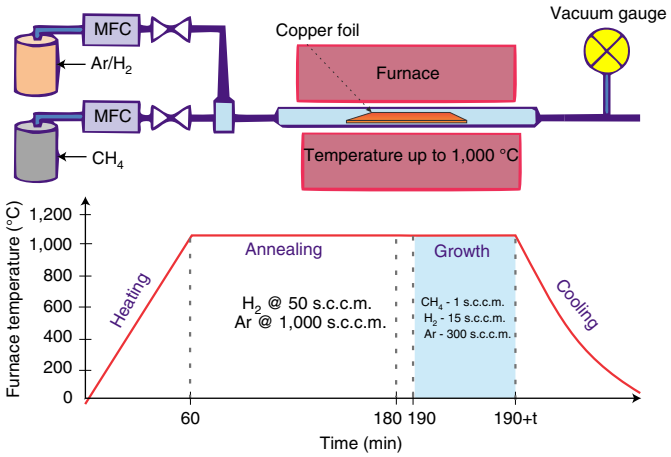

Fig. 4 | Schematics of the CVD growth process and an approximate timeline recipe for graphene growth. A typical CVD graphene growth setup consists of a chamber or quartz tube, heated to ~1,000 °C, connected to carrier gas (e.g., Ar/H_2) and carbon-containing gas (e.g., CH_4) via mass flow controllers (MFC). The lower part of the figure illustrates a typical graphene growth recipe.

- Hioki LCR Sample Application (https://www.hioki.com/en/support/versionup/detail/?downloadid=257)
- Hioki HiTESTER for older LCR models (https://hiokiusa.com/support/application-software-for-lcr-hitester/)
- Open BCI GUI (https://openbci.com/index.php/downloads)
- Origin Pro for data analysis and plotting (https://www.originlab.com/origin)
- Silhouette Software (https://www.silhouetteamerica.com/software)
- MS Excel (https://www.microsoft.com/en-us/microsoft-365/excel)

Procedure

(Optional) CVD growth of graphene ● Timing 3–4 h

▲ **CRITICAL** This section can be skipped if commercially available CVD-grown graphene on copper foil is used instead (see Reagents).

1 Pre-clean the copper foil in nitric acid. The dimensions of the copper foil should be such that it can fit to the CVD reactor furnace, varying from 1–2 inches in laboratory conditions and 4–8 inches in industrial setups. Commonly used in this work are graphene/copper foils of 2 × 2 inches.
! CAUTION Nitric acid is harmful if swallowed and can cause skin irritation and eye damage. Wear gloves and safety glasses when handling.

2 Load copper foil into the CVD growth furnace (e.g., Black Magic, Aixtron), evacuate and elevate temperature to ~1,000 °C for 2 h for annealing. Gas composition: 1,000 s.c.c.m. Ar, 50 s.c.c.m. H_2 (see Fig. 4).

3 Introduce CH_4 at 1 s.c.c.m. into the chamber to start the growth. Change Ar to 300 s.c.c.m. and H_2 to 15 s.c.c.m.

4 After ~10 min of growth turn the CH_4 gas off, cool down and vent the chamber.
■ PAUSE POINT The CVD-grown graphene can be stored for years at room temperature and preferably in vacuum-sealed conditions to prevent copper oxidation.

5 Check quality of the CVD-grown graphene in a nondestructive manner, using Raman spectroscopy. See Box 2 for details on how to determine graphene quality from Raman spectra.

Preparation of graphene/copper foil for transfer ● Timing 30 min

6 In order to protect graphene during the subsequent Cu etch and processing, the graphene/Cu stack (Fig. 5a) has to be covered with PMMA. Place the copper foil on top of a dummy Si wafer and carefully cover the edges with Kapton scotch tape or any other cleanroom-suitable tape (see Fig. 5b).
▲ **CRITICAL STEP** If the tape is not well in contact with the foil, the PMMA can reach underneath the copper foil, impairing the ability to etch copper in the following steps completely.

7 Spin-coat a layer of PMMA (950 A4) at a rate of ~2,500 r.p.m. for 60 s to result in a ~200-nm-thick layer (see Fig. 5c).

8 Soft bake on a hotplate at 200 °C for 15–20 min. At such a high temperature, PMMA overcomes the glass transition to ensure its mechanical and chemical stability during further processing.

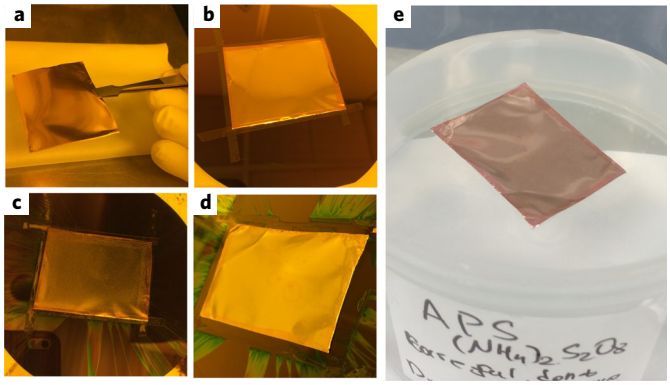

Fig. 5 | Preparation of the copper foil (Steps 1–4). Bare copper foil with graphene grown on top (**a**), fixed with Kapton tape on the edges (**b**), spin-coated with PMMA on top and hard-baked (**c**), released from Kapton tape (**d**), and finally placed into a copper etchant (**e**).

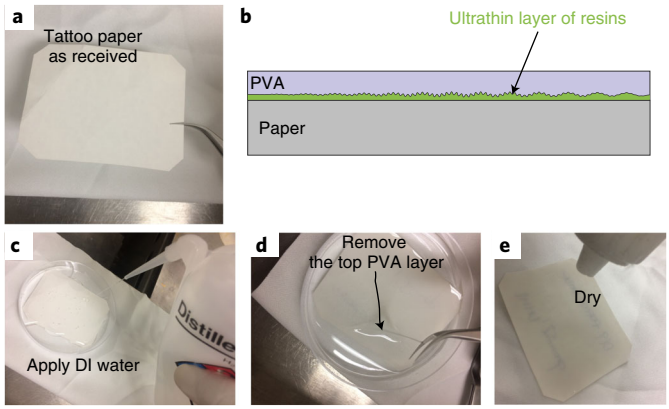

Fig. 6 | Preparation of a bare tattoo substrate (Steps 6–9). a, Temporary tattoo paper as received, with an ultrathin layer of hydrophobic PVA coverage on top and a layer of resin epoxies (green) that make the paper slippery when wet (**b**). Once the water is applied to the paper (**c**), the hydrophobic PVA can be easily peeled off the paper's surface by picking it up with tweezers (**d**). The final paper can be dried if extended storage is required (**e**).

▲ **CRITICAL STEP** Make sure the hot plate is calibrated and the temperature does not go above 200 °C, as it will cause degradation of the PMMA and, consequently, of the final device.

? TROUBLESHOOTING

9 Carefully remove the Kapton tape (see Fig. 5d).

▲ **CRITICAL STEP** For very thin copper foils, avoid excessive bending, crumpling and rupturing of the copper foil that can be caused by the tape removal.

■ **PAUSE POINT** PMMA-capped graphene on copper foil can be stored for months at room temperature without graphene quality degrading.

? TROUBLESHOOTING

Preparing tattoo paper for transfer ● Timing 10 min

▲ **CRITICAL** The tattoo paper (see Fig. 6a), as received from the supplier, has several polymers on top of the paper itself. The topmost layer is the ultrathin PVA, which is hydrophilic, water dissolvable and detaches from the paper when wet, hence it must be removed from the paper stack before use. Under the PVA there is a thin layer of resins (polyamide, polyalyl and polyurethane, see Fig. 6b). The resin layer makes the paper slippery when wet and sticky when dry.

10 The PVA layer is unfavorable for our process and must therefore be removed. To remove the PVA, simply dip the paper into DI water (see Fig. 6c). Wait 10–30 s for the water to soak the whole paper. Prepare two pieces of paper for each tattoo. One of those will serve as a ***source*** paper, and it is used to fish out the floating PMMA/graphene stack in Step 17. The source paper should be slightly larger than the size of the PMMA/graphene piece. The second one will be the ***target*** paper. For best

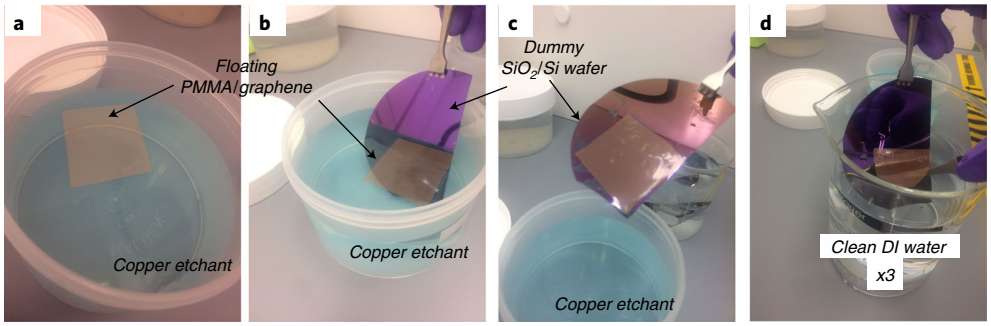

Fig. 7 | Transfer of PMMA/graphene flake from the copper etchant (light blue) into clean DI water (Steps 13–15). **a**, The PMMA supported graphene floating on the surface of the copper etchant after the etching is finished. Here and later on, the PMMA/graphene is highlighted in dark opaque orange color as a guideline because the optical contrast is rather low. Using a clean SiO_2/Si piece, dip it into the solution (**b**) and fish out the PMMA/graphene flake (**c**). Then carefully lower the silicon wafer with PMMA/graphene into a beaker with fresh, clean DI water (**d**). Repeat ≥3 times with clean DI water.

results, it should be even larger (5–10 mm on each side) than the ***source*** paper. Examples of the **target** and **source** papers are shown in Fig. 8a,b.

? TROUBLESHOOTING

11 Carefully scratch and pick the PVA layer and pull up. It is strong enough to sustain itself and should not break apart (see Fig. 6d).

12 The paper can now be dried out and used later any time whenever required.

■ PAUSE POINT The paper can be stored at room temperature for years. Before using the completely dried paper, simply dip it in water for 60 s before use.

Transferring graphene onto tattoo paper ● Timing 30 min + 12 h wait

13 Prepare the 0.1 M copper etchant solution by mixing 22.8 g of $(NH_4)_2S_2O_8$ powder with 1 liter of DI water. Place the copper foil from Step 9 into the copper etch solution $(NH_4)_2S_2O_8$ for at least 8–12 h.

! CAUTION Ammonium persulfate is corrosive. Wear personal protective equipment and work in a fume hood.

▲ CRITICAL STEP Removing or not removing the backside graphene generates GETs without or with graphene nanoscrolls, respectively (see Box 2 for details).

? TROUBLESHOOTING

14 By using a piece of Si wafer (must be larger than the piece of PMMA/graphene flake), slowly and carefully pick up the floating PMMA/graphene onto the wafer (Fig. 7a–c) and transfer into DI water (see Fig. 7d). Wait 5–10 min.

15 Transfer the PMMA/graphene into a second beaker with fresh DI water (see Fig. 7d). Wait for 10 min, move into a new clean DI water, repeat three times. This is essential to keep the graphene interface clean, without copper etchant residues. Let the piece float for ≥20 min in the final water wash.

▲ CRITICAL STEP Try not to damage the film during the multiple transfer steps. Use a fresh SiO_2/Si piece for every transfer. Since the graphene will later be in contact with human skin, it is of absolute importance to have the surface free of contaminants.

16 If both the ***source*** and ***target*** tattoo papers were prepared ahead of time (see Steps 10–12) and are already completely dry, immerse them in DI water in a different container and let the papers soak for 1 mi). ***Source*** paper is ready to use when entirely wet. However, the ***target*** paper needs additional treatment. Take it out of the water, place on a piece of tissue, and blow-dry its surface to remove excess water from the top surface at room temperature.

▲ CRITICAL STEP If the ***target*** paper is completely wet, it creates a thick water barrier to the PMMA/graphene, resulting in a failure to transfer. Conversely, if the ***target*** paper is 100% dry, the process will also fail due to a lack of adhesion forces between the dry paper and the PMMA/graphene piece.

17 Fish the PMMA/graphene stack from the beaker containing DI water (from Step 15) with the ***source*** tattoo paper.

? TROUBLESHOOTING

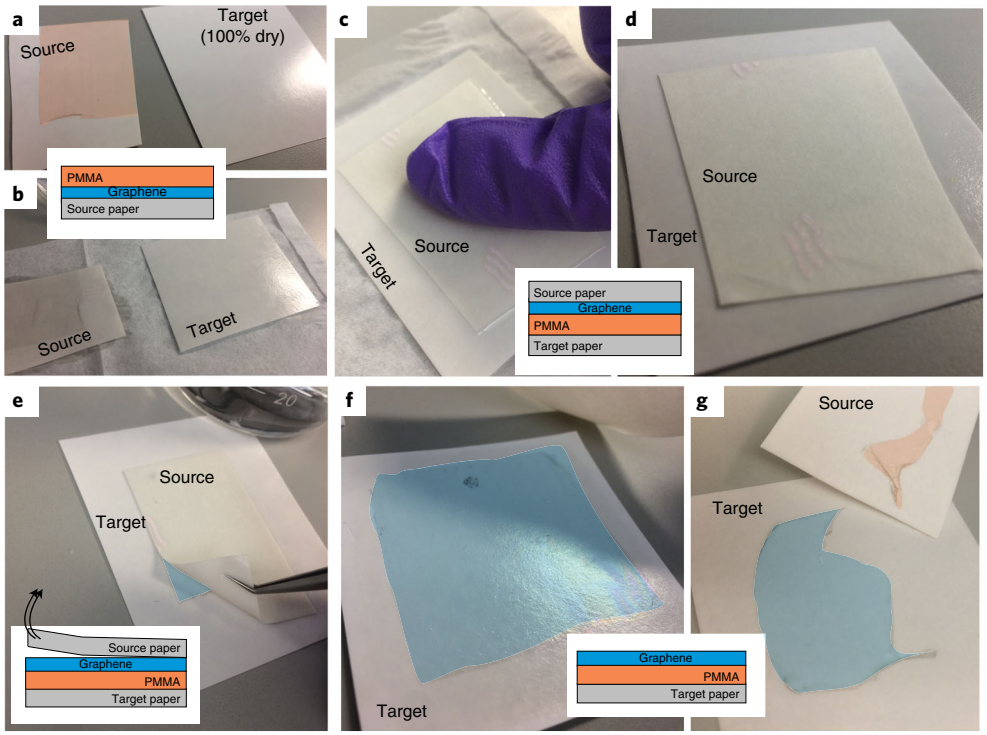

Fig. 8 | The graphene flip process (Step 18). a,**b**, The source (left, with PMMA on top) and target (right) papers prepared as described in Steps 10–12. **c**,**d**, The target and source papers are brought into contact, and slight pressure is applied from the top. **e**, The beginning of the source paper's delamination. **f**, Successful delamination. **g**, Less successful example of the transfer process. Insets next to each subfigure show the precise topography of the PMMA, graphene, and paper for each case. Throughout the figure, whenever the PMMA is facing up, the area is highlighted orange; if the graphene is facing up, the area is highlighted blue.

18 Place the ***source*** paper (with PMMA/graphene) upside down on the ***target*** tattoo paper. Carefully apply pressure, making sure not to slide the two pieces around (see Fig. 8c). Apply several drops of DI water on top of the stack to keep the top ***source*** paper wet without introducing too much water to the interface between the papers. Make sure that there is a tissue under the target paper to soak the excess of liquid (see Fig. 8d). Within 1 min, carefully peel the source tattoo paper off the target, which should leave the graphene/PMMA stack on top of the target paper (see Fig. 8e,f). See Supplementary Video 1 for visual aid.

▲ **CRITICAL STEP** This step is essential to reverse the positions of PMMA and graphene, so that when further transfer on top of the tissue is done, the graphene will be facing the tissue. If the process fails (see Fig. 8g for an example), the transfer can be repeated for the unreversed piece. This is perhaps the most critical step enabling success of the whole protocol, and we strongly suggest watching Supplementary Video 1 for a complete understanding.

? TROUBLESHOOTING

19 Let the paper dry out completely before proceeding to the next step. Dry for at least 8–12 h at room temperature.

■ **PAUSE POINT** The graphene/PMMA/paper stack can now be stored at room temperature in a dry and dust-free environment for years.

Cutting GETs ● Timing 1 h

20 Prepare the Cameo plotter or any other mechanical cutter machine. Once the PMMA/graphene/tattoo has dried completely, cut it into the desired shape. In the case of the cameo silhouette machine, it is possible to set different depth parameters for the process. Typically, a depth of '3' (an internal setting) would result in a deep cut through the whole paper. However, in our experience, this only complicates the subsequent steps of the procedure. Therefore, it is recommended to only ***scribe*** the surface by selecting a cut depth of '1', slowest possible speed, and only a single cut.

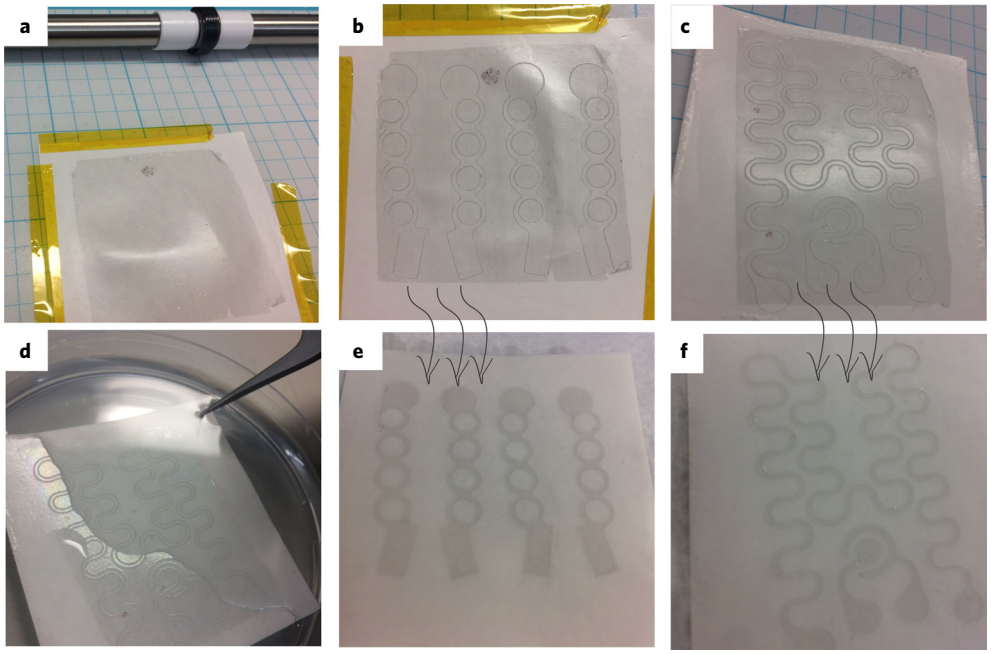

Fig. 9 | Shaping GETs via the cameo plotter (Steps 20–22). a, A piece of graphene/PMMA/tattoo paper fixed on a cutting mat ready for the dicing process. **b**,**c**, The outcomes of the cutting process (two different shapes). **d**, The process of PMMA/graphene excess removal. **e**,**f**, The results of the structures cut in **b** and **c**, respectively.

▲ **CRITICAL STEP** The cut should be deep enough to cut through the top layer, but should not cut through the whole material.

? TROUBLESHOOTING

21 Use a non-sticky cutting mat to ensure the back side of the tattoo paper is not damaged, and use Kapton tape to firmly attach the edges of the piece of PMMA/graphene/tattoo onto the cutting mat to ensure that the paper will not slide aside during the process (see Fig. 9a). Supplementary Video 2 shows the process.

22 Once the desired shape is scribed (see examples in Fig. 9b,c), immerse the graphene/PMMA/tattoo into fresh DI water for at least 1 min. After immersion, use tweezers to carefully remove the parts of the design that should not be transferred afterward (see Fig. 9d,f and Supplementary Video 3 for details). It is a rather straightforward process that is enabled by a weak adhesion between the PMMA and the paper (due to the presence of resins on the paper's surface) and the mechanical stability of the PMMA film. Once the excess PMMA/graphene is removed, the design is ready to be transferred to the tissue.

■ **PAUSE POINT** The design can be transferred to the tissue immediately, or dried and stored at room temperature in a dry and dust-free environment for months up to years without any degradation.

23 (Optional) Passivate parts of the graphene if needed for specific applications. If the tattoo design is complex/large, it might be essential to localize the measurements via passivating some parts of the device, leaving other parts open. This can be done by shadow masking (regular paper will suffice) and spraying Nexcare liquid bandage on top. Alternatively, Tegaderm can be used as a temporary layer that provides local passivation and eases the connections.

Transferring GETs to skin and assembling the readout ● Timing 1 h

! CAUTION Experiments with human subjects should be performed in accordance with national and institutional regulation and require informed patient consent. The human subject experiments described herein were performed under UT Austin Institutional Review Board approval #2018-06-0058.

24 To provide electrical contact to the graphene tattoo while enabling it to form an imperceptible contact with skin, we developed two approaches. Both utilize ultrathin soft adhesive conductive tape as the intermediary (see Box 3). In order to connect the GET to electronics using copper tape, follow Option A. For soldering via silver epoxy, follow Option B.

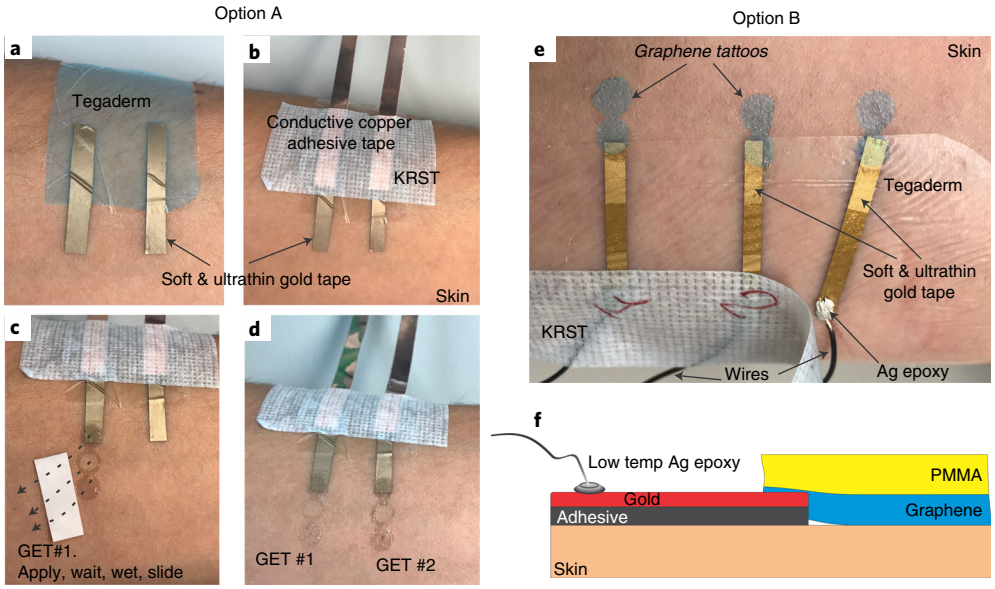

Fig. 10 | Placement of conductive wires and transfer of GETs. Step 24, Option A: **a**–**d**, Tegaderm is applied as a passivation and protection layer, and the strips of soft conducting tape applied partially on top of the Tegaderm (**a**). The firm adhesive conductive copper tape is applied on top of the soft conductive tape and sealed with KRST to ensure physical stability (**b**). The transfer of two GETs is shown schematically in **c** and **d**. Step 24, Option B: **e** differs from the previous procedure only by low-temperature silver epoxy-enabled direct connection with wires (**f**).

(A) **Contact using copper tape**

▲ **CRITICAL** See Supplementary Video 4 for visual aid.

(i) Place a small patch of Tegaderm on the skin (the area to be covered with metal connectors and Cu tape, see Fig. 10a).

(ii) Place the soft metal connectors (fabricated and assembled as described in Box 3) onto the skin, on the area where the GET's connector area will be located.

(iii) For better stability and robustness of the connection, place the adhesive double-sided conductive copper tape as an intermediate between soft tape and electronics.

(iv) (Optional) In order to ensure physical balance, the connector area can be tightened with 3M Kind Removal Silicone Tape (see Fig. 10b).

(B) **Contact using silver epoxy**

▲ **CRITICAL** See Supplementary Video 5 for visual aid.

(i) Place a small patch of Tegaderm on the skin.

(ii) Prepare the soft conductive tape (fabricated and assembled as described in Box 3) by gluing one side of it to a wire via conductive silver epoxy glue. Place these pre-assembled connectors onto the edge of the Tegaderm (see Fig. 10e,f).

(iii) (Optional) In order to ensure physical balance, the connector area can be tightened with 3M Kind Removal Silicone Tape (see Fig. 10e).

25 Soak the graphene/PMMA/tattoo paper from Step 22 in DI water for at least 10–20 min. When ready, remove from the water, carefully touch it with the side of a paper tissue to remove any excess of water, then place it onto the skin, aligned to the previously placed soft conductive tape. Apply slight pressure and wet the tattoo with a small drop of DI water (similar to Step 18). The soaking, transfer and optional troubleshooting steps (see below) do not change the electrical qualities of the GETs.

▲ **CRITICAL STEP** Carefully begin sliding the paper away then release the paper, leaving the graphene/PMMA in direct contact with the skin (see Fig. 10c,d). In case where the tattoo does not simply slide off and sticks to the paper, please refer to the troubleshooting table and see Supplementary Video 6 for a detailed visual aid for this process and the most common troubles with the transfer. Wait 30–60 s to dry out.

? TROUBLESHOOTING

26 (Optional) In order to ensure stable operation, it is possible (only if long-term, >12h tattoo operation is planned) to apply a layer of liquid bandage by directly spraying it onto the graphene/skin area and allowing 30 s to dry out.

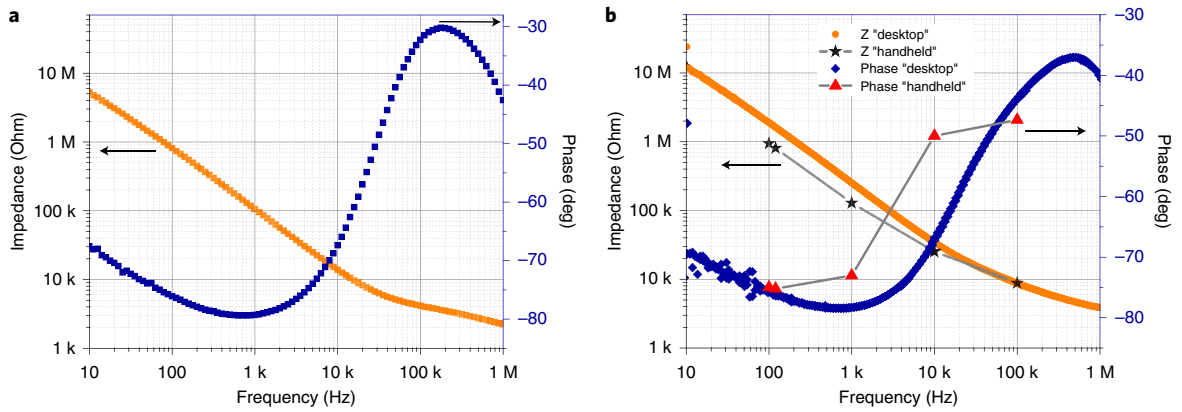

Fig. 11 | Electrical performance of the GETs on skin. A typical GET's impedance and phase dependency over frequency (**a**) and comparison (**b**) of the data recorded via a high-end desktop LCR meter (orange and blue symbols) vs. low-end handheld LCR meter (black stars and red triangles). Arrows pointing left or right represent which of the plots belong to the left (impedance) or right (phase) *y* axis.

Measurements

27 For skin impedance tests, follow Option A. For skin hydration monitoring, follow Option B. For temperature monitoring, follow Option C. For low-cost EEG, EMG, or ECG monitoring, follow Option D.

(A) **Skin impedance test** ● Timing **1 h**

(i) Connect a pair of GETs to either a handheld or a desktop LCR meter. Measure impedance (its real and imaginary parts) while varying the frequency of the carrier AC signal. A typical output plot of impedance amplitude and phase with high resolution in sampling frequency is shown in Fig. 11a. If a lower quality, handheld LCR meter is used with a limited frequency range, the skin contact impedance plot can still be measured with a reasonable quality, as shown in Fig. 11b.

▲ CRITICAL STEP To obtain more data for statistical purposes, place three similar tattoos (A, B, C) at once and measure three different impedance combinations (A–B, A–C and B–C), then take half of each value to calculate the average.

(ii) Read out the impedance value at 10 kHz (figure of merit). Divide by two in order to calculate the impedance value per tattoo. As shown in Fig. 11b, the final values of the skin impedance at ~10kHz frequency can be finely estimated even with low-end handheld LCR meters.

(B) **Skin hydration monitoring** ● Timing **1 h**

(i) Place at least one pair of GETs on the skin and perform an impedance sweep. Depending on the equipment (e.g., handheld LCR meter or desktop LCR meter) settings, there are two possible recording strategies:

- Set a constant frequency and perform timetrace measurements, recording the change in impedance amplitude over time.
- Set the measurement sweep into a fast mode (5–10 s per whole sweep range) and perform a continuous sweeping to record the changes of the complex impedance at the entire frequency range (see an example in Fig. 2c,d).

(ii) Tune the skin hydration level by applying a body lotion, spraying water on top or simply inducing conditions that would enable extensive sweating.

(iii) Perform a set of the contact impedance measurements over an extended time, while monitoring skin hydration in parallel via a commercially available tool (e.g., MoistureMeterSC). Correlate and check for impedance changes over the hydration level.

(iv) Once the calibration (see Step iii) is performed, the tattoo can stay on the body for a longer time, and a simple impedance sweep will measure skin hydration level.

(C) **Temperature monitoring** ● Timing **1 h**

(i) Prepare a serpentine or strip-shaped GET and transfer onto skin with two electrodes connecting the sides of the strip.

(ii) Using either a handheld source meter (e.g., LCR meter set in DC Resistance mode) or a complex SMU system (e.g., Keysight B2902A), drive a current/voltage through the graphene and measure the corresponding voltage/current to calculate the resistance of the GET. Set the tool for continuous timetrace monitoring mode.

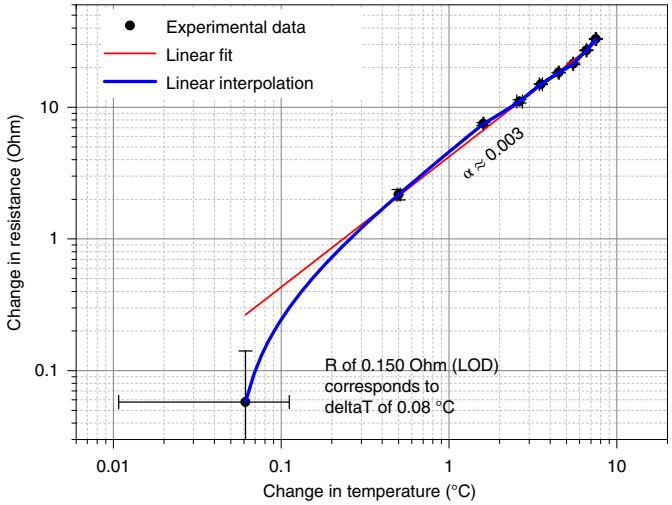

Fig. 12 | A typical biGET's temperature response. Black circles represent the experimental data, while the red and blue lines represent linear fit and interpolation.

(iii) While monitoring a GET's resistance over time, place a commercially available thermocouple near the tattoo to calibrate the tattoo's temperature coefficient of resistance. See Fig. 2a and Fig. 12 for examples of the GET's temperature response and calculated limit of temperature detection, ~0.08 °C.

(iv) Once the GET's base temperature sensor is calibrated, resistance changes will be directly related to body temperature changes. The thermocouple can be removed, and the resistance change of the graphene thermistor can be directly correlated to the change in temperature.

(D) **Low-cost EEG, EMG, or ECG monitoring** ● **Timing 30+ min**

(i) Place the required number of GETs onto relevant locations depending on the specific application:

- ECG monitoring: requires ≥2 GETs to be placed onto the subject. Two of the most common electrode locations for ECG monitoring are on the chest as close to the heart as possible or on the two forearms, with one tattoo on each arm. The ECG measurements are taken differentially, so generally the larger the spacing between two electrodes the better the signal quality. The reference electrode here can be placed by the right abdomen.
- EMG monitoring: requires a pair of tattoos placed over a muscle with the signal being read out differentially. The muscular contractions will result in the generation of a net electrical potential that is recorded by the tattoo pair. The EMG monitoring tattoos can be placed over the muscle of choice. Due to small lateral dimensions and intimate contact to skin, GETs can be used for precise muscle activity monitoring and building complex HMIs. The reference electrode for EMG monitoring can be placed near a bone, e.g., by the elbow when focusing on arm muscles.
- EEG monitoring: requires graphene tattoos to be placed on the subject's head. The most accessible part for successful GET placement is the forehead, specifically Fp1 and Fp2 locations. The reference electrode in this configuration is best placed close to the bone, typically behind one's earlobe.

(ii) Following the instructions at https://docs.openbci.com/docs/01GettingStarted/01-Boards/GanglionGS for installation and software usage, connect the tattoos to the appropriate pins on the electrophysiological data monitoring board.

▲ **CRITICAL STEP** Either the Ganglion Open BCI board or the Cyton Open BCI board can be used (see Fig. 13). While Cyton allows for ≤8 channel simultaneous measurements, we found the Ganglion board, with only four channels, sufficient for proof-of-principle operation.

(iii) In the ECG, EMG and EOG monitoring cases, connect the GETs in pairs and set them up in a differential amplification mode. Such a design allows simultaneous measurements from as many as four GET pairs. An example of ECG monitoring with the Ganglion board and resulting cardiac timetraces is shown in Fig. 13.

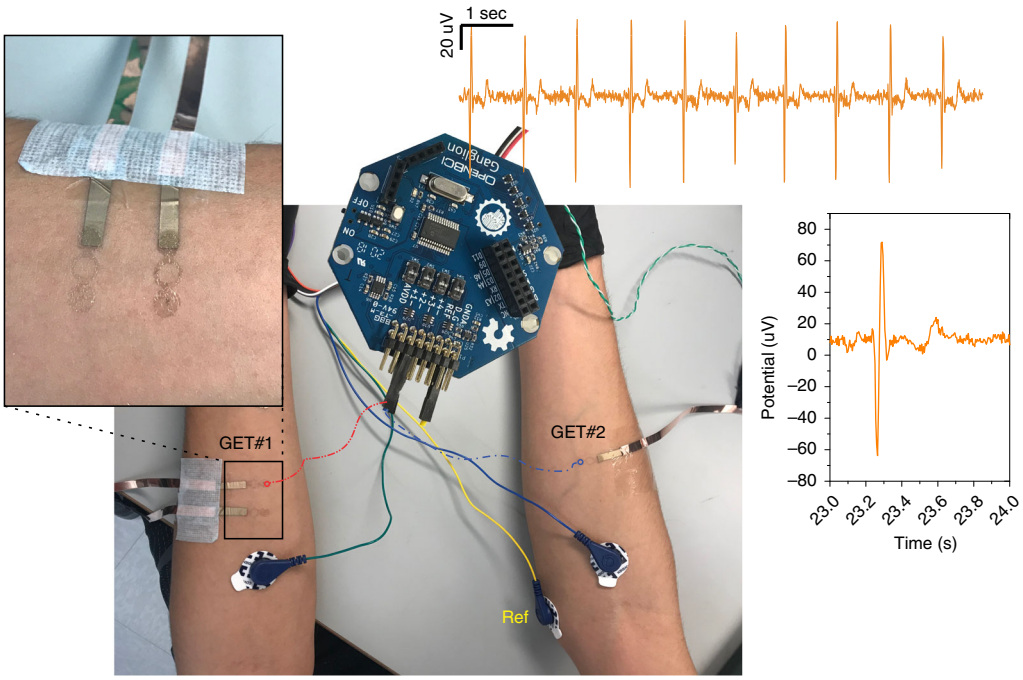

Fig. 13 | ECG measurement setup via Open BCI ganglion board. This setup features two GETs on the left hand (only one connected) and one GET on the right hand with the differential measurement performed. Another pair of Ag/AgCl gel electrodes are used for signal comparison and confirmation. The ECG waveform is shown at the top right.

(iv) In the case of EEG monitoring, there is no need to use specific pairs of electrodes for each channel. Instead, place one single reference (REF) electrode, which will be bundled up and connected to all four electrodes.

Troubleshooting

Troubleshooting advice can be found in Table 1.

Table 1 | Troubleshooting table

Step	Problem	Possible reason	Solution
8	PMMA is black, and copper seems oxidized	PMMA did not get coated uniformly	Flatten the copper foil before PMMA spin-coating; spin-coat PMMA twice
		Hot plate temperature too high	Double-check the hot plate temperature
9	Copper foil is bent and damaged	The forces applied during tape removal pulled the sides of copper foil	The tape must be removed by pulling it at almost a 180° angle to the surface
10	Paper bent up during water immersion	Surface tension difference	The paper will flatten out once the PVA is detached and removed
13	Copper is not fully etched	PMMA got underneath the copper foil	Make sure the tape is tightly attached to the edges (Step 6)
		Air bubble formed during etching or placing onto etchant	Pick up the flake with the dummy wafer and transfer into water and back; the bubble should be gone. If it is not, repeat
		Cu etchant is saturated (vibrant blue color)	Exchange the etchant
17	PMMA/graphene flake is repelled during transfer	The paper was not soaked well enough or soaked in a saturated water	Clean each of the **source** papers in fresh water for best results
	PMMA/graphene is sliding off while fishing it out	The layer of resins on the paper makes it slippery, and is essential for the whole process	Use two wide tweezers. Use one to hold the paper; use the other tweezer to push the flake to assist the transfer

Table continued

Table 1 (continued)

Step	Problem	Possible reason	Solution
18	PMMA/graphene does not stick to **target** paper and stays on **source** paper	Too much water on top of the **target** paper	Make sure the **target** paper has no water on top of it
		Not enough adhesion to the target paper	Make sure to apply pressure and liquid on top of the source paper before attempting delamination. Do not apply shear forces; try to delaminate from a corner until it goes along. If it does not, try another corner. Try to slide off before peeling off
20	Cutting results in a complete scratch of the material instead of clean cut	Paper is still wet	Make sure the paper is completely dry. Usually 2–3 h is not enough; dry for at least 8–12 h. Make sure the room humidity allows the paper to dry out
		Wrong cutting settings	Check and adjust the settings
		Wrong, damaged or dirty blade or blade holder	Check, clean and exchange the blade frequently
25	Tattoo does not get transferred onto the skin	Too much water on the skin	Simply dry out the skin and repeat
		Not enough pressure applied	Apply more pressure and wait a bit longer
		Adhesion to the tattoo paper is too high	An easy trick is to dry the tattoo paper on the edge of a tissue paper, and re-immerse back into the water slowly and carefully. See if the tattoo paper starts to delaminate at the interface with water. If not – repeat until you see delamination. If delamination occurs, the GET will be transferred onto the skin with a 100% yield. One can prolong the shelf life of such 'prepared' tattoos by keeping them on a bed of wet tissue

Timing

Steps 1–5, (Optional) CVD growth of graphene: 3–4 h
Steps 6–9, Preparing graphene/copper foil for transfer: 30 min
Steps 10–12, Preparing tattoo paper for transfer: 10 min
Steps 13–19, Transferring graphene onto tattoo paper: 30 min + 12 h
Steps 20–23, Cutting GETs: 1 h
Steps 24–26, Transferring GETs to skin and assembling the readout: 1 h
Step 27, Option A, Measurements, skin impedance check: 1 h
Step 27, Option B, Measurements, skin hydration monitoring: 1 h
Step 27, Option C, Measurements, temperature monitoring: 1 h
Step 27, Option D, Measurements, low-cost EEG, EMG, or ECG monitoring: ≥30 min

Anticipated results

Perhaps the most crucial issue that had to be resolved in the development of this protocol was to ensure the reproducibility of the results in terms of the tattoo's electrical performance. Typically, when using monolayer GETs, electrical properties such as sheet resistance and impedance vary substantially (see Fig. 14). One device can have excellent performance; another one, taken from precisely the same graphene batch, can be two- or even fivefold worse. We attribute this to the monolayer graphene's structural inconsistency when a single crack or inhomogeneity coming from the CVD growth or transfer can result in whole device degradation. Moreover, when comparing pure monolayer graphene samples (with backside graphene etched) to monolayer graphene with graphene nanoscrolls (without etching away the backside graphene, see Box 2), we find that the GET + nanoscrolls result in a better and more repeatable performance, perhaps due to the nanoscrolls bridging the graphene grains, reinforcing electrical homogeneity.

In order to directly compare the quality of different graphene sources, we performed a sampling study, using graphene from three suppliers—Grolltex, Cqmxi and research-grade material from collaborating partners—making monolayer, bilayer and trilayer tattoo structures out of each

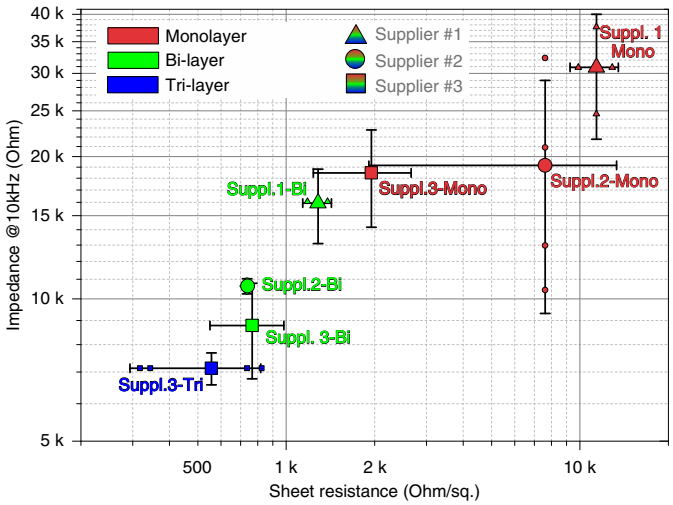

Fig. 14 | Impedance vs. sheet resistance comparison for mono- (red), bi- (green), and tri- (blue) layer configurations of graphene from three different suppliers (triangle, circle, and square). For most of the cases, the number of samples used for each of the impedance and Rs tests was >6. However, in the case of Suppliers (Suppl.) 1 and 2, as well as when creating trilayer GETs with Supplier 3, the overall number of samples tested was 2–4, and those individual values are shown as smaller points (see small black squares, green tiangles, and red circles and triangles).

graphene. The bilayer and trilayer samples are fabricated as described in Box 2. Because a pair of GETs is required to measure skin impedance, the impedance value is then divided by two in order to yield a value of impedance per graphene tattoo. We transferred ≥3 GETs (A, B, C) and measured impedance in all three combinations, divided by two, and averaged the values to yield statistically relevant data. The number of tested GETs of each kind was ≥10 and reached up to 50 in the case of the third supplier (Fig. 14). Sheet resistance was measured by placing a strip of GET out of the same batch onto an Ecoflex-covered glass frame with four soft conductive gold electrodes. This is done to reproduce skin-like texture and softness as precisely as possible. Four-point transmission line method (TLM)-based measurements were performed to estimate sheet resistance. The values reported are averages from at least two or three strips of each kind. Noteably, as seen in Fig. 14, regardless of the source of graphene, the monolayer usually yields much lower performance in terms of both skin impedance and sheet resistance. In terms of sheet resistance, the monolayer GETs vary from 2kΩ/sq. to 12 kΩ/sq. In regard to skin impedance, there are occasionally good samples of the monolayer GETs (~10 kΩ of skin impedance), but the overall statistical distribution is too large, and the next sample from the exact same batch might result in poor performance (≤40 kΩ). Bilayer GET structures have been found to have average skin impedance in the range of 8–10 kΩ (third supplier), and outstanding sheet resistance, below 1kΩ/sq. The large values of electrode-skin impedance are not of general importance for some tasks such as EMG or ECG monitoring since the electronics can be fine-tuned to fit the impedance of the electrodes. However, for advanced applications, it is essential to ensure that GET performance does not vary drastically from one tattoo to another, and that electrode-skin impedance is as low as possible to enable current injection.

In conclusion, while trilayer samples result in even more superior performance, the efforts required to fabricate trilayer GETs perhaps cancel out the feasibility of using tri-GETs on a regular basis. Hence, we propose that bi-GETs, due to their balanced combination of fabrication efforts and electrical, optical and mechanical properties, are arguably the most suitable option for wearable electronics in the future. Moreover, the current scale of industrial graphene fabrication (see supplementary Table 2), suggesting prices as low as US$0.5 per cm^2 of graphene, is only the beginning. There are technologies available to further scale up graphene growth production, lowering the prices by orders of magnitude, whenever market requirements will be met by demand. We believe that GETs and their potential use for personalized medicine is an extremely promising application of graphene and, if widely adopted, the technology can help drive the costs of graphene down. Furthermore, the whole procedure described here, including graphene growth, polymer coating, copper etch, transfer, mechanical cutting (or laser cutting in the future) and even transferring graphene from source to target paper can be industrialized, automated and scaled up.

Reporting Summary

Further information on research design is available in the Nature Research Reporting Summary linked to this article.

Data availability

Source data are provided with this paper.

References

1. Flores, M., Glusman, G., Brogaard, K., Price, N. D. & Hood, L. P4 medicine: how systems medicine will transform the healthcare sector and society. *Per. Med.* **10**, 565–576 (2013).
2. Becker, S. et al. mHealth 2.0: experiences, possibilities, and perspectives. *JMIR mHealth uHealth* **2**, e24 (2014).
3. Chow, C. K., Ariyarathna, N., Islam, S. M. S., Thiagalingam, A. & Redfern, J. mHealth in cardiovascular health care. *Heart Lung Circ.* **25**, 802–807 (2016).
4. Price, M. et al. mHealth: A mechanism to deliver more accessible, more effective mental health care. *Clin. Psychol. Psychother.* **21**, 427–436 (2014).
5. Ray, T. R. et al. Bio-integrated wearable systems: a comprehensive review. *Chem. Rev.* **119**, 5461–5533 (2019).
6. Mukhopadhyay, S. C. Wearable sensors for human activity monitoring: a review. *IEEE Sens. J.* **15**, 1321–1330 (2015).
7. Heikenfeld, J. *et al*. Wearable sensors: modalities, challenges, and prospects. *Lab Chip* **18**, (2017).
8. Neethirajan, S. Recent advances in wearable sensors for animal health management. *Sens. Bio-Sensing Res* **12**, 15–29 (2017).
9. Guk, K. et al. Evolution of wearable devices with real-time disease monitoring for personalized healthcare. *Nanomaterials* **9**, 1–23 (2019).
10. Wearable Technology Market—Growth, Trends, and Forecasts (2020–2025). https://www.researchandmarkets.com/reports/4591296/wearable-technology-market-growth-trends-and
11. Wang, C. et al. Monitoring of the central blood pressure waveform via a conformal ultrasonic device. *Nat. Biomed. Eng.* **2**, 687–695 (2018).
12. Kim, D.-H. et al. Epidermal electronics. *Science* **333**, 838–843 (2011).
13. Gutruf, P. et al. Fully implantable optoelectronic systems for battery-free, multimodal operation in neuroscience research. *Nat. Electron.* **1**, 652–660 (2018).
14. Miro, P. et al. An atlas of two-dimensional materials. *Chem. Soc. Rev.* **43**, 6537–6554 (2014).
15. Ferrari, A. C. et al. Science and technology roadmap for graphene, related two-dimensional crystals, and hybrid systems. *Nanoscale* **7**, 4598–4810 (2015).
16. Chhowalla, M., Jena, D. & Zhang, H. Two-dimensional semiconductors for transistors. *Nat. Rev. Mater* **1**, 16052 (2016).
17. Bhimanapati, G. R. et al. Recent advances in two-dimensional materials beyond graphene. *ACS Nano* **9**, 11509–11539 (2015).
18. Kireev, D., Offenhaeusser, A. & Offenhäusser, A. Graphene & two-dimensional devices for bioelectronics and neuroprosthetics. *2D Mater* **5**, 042004 (2018).
19. Hess, L. H., Seifert, M. & Garrido, J. A. Graphene transistors for bioelectronics. *Proc. IEEE* **101**, 1780–1792 (2013).
20. Kireev, D. et al. Graphene transistors for interfacing with cells: towards a deeper understanding of liquid gating and sensitivity. *Sci. Rep.* **7**, 6658 (2017).
21. Kireev, D. et al. Graphene multielectrode arrays as a versatile tool for extracellular measurements. *Adv. Healthc. Mater.* **6**, 1601433 (2017).
22. Kabiri Ameri, S. et al. Graphene electronic tattoo sensors. *ACS Nano* **11**, 7634–7641 (2017).
23. Ameri, S. K. et al. Imperceptible electrooculography graphene sensor system for human–robot interface. *npj 2D Mater. Appl.* **2**, 19 (2018).
24. Sel, K. *et al*. Electrical characterization of graphene-based e-tattoos for bio-impedance-based physiological sensing. *BioCAS 2019 - Biomed. Circuits Syst. Conf. Proc.* 1–4 (2019). https://doi.org/10.1109/BIOCAS.2019.8919003
25. Zhang, X. et al. Ultrasensitive field-effect biosensors enabled by the unique electronic properties of graphene. *Small* **16**, 1902820 (2020).
26. Huang, H. et al. Graphene-based sensors for human health monitoring. *Front. Chem.* **7**, 1–26 (2019).
27. Wassei, J. K. & Kaner, R. B. Graphene, a promising transparent conductor. *Mater. Today* **13**, 52–59 (2010).
28. Das, T., Sharma, B. K., Katiyar, A. K. & Ahn, J.-H. H. Graphene-based flexible and wearable electronics. *J. Semicond.* **39**, 011007 (2018).
29. Park, D. et al. Fabrication and utility of a transparent graphene neural electrode array for electrophysiology, in vivo imaging, and optogenetics. *Nat. Protoc.* **11**, 2201–2222 (2016).
30. Song, J.-K. et al. Wearable force touch sensor array using a flexible and transparent electrode. *Adv. Funct. Mater.* **27**, 1605286 (2017).
31. Yang, S. et al. "Cut-and-paste" manufacture of multiparametric epidermal sensor systems. *Adv. Mater.* **27**, 6423–6430 (2015).

32. Wang, Y. et al. Low-cost, μm-thick, tape-free electronic tattoo sensors with minimized motion and sweat artifacts. *npj Flex. Electron.* **2**, 6 (2018).
33. Stier, A. et al. Stretchable tattoo-like heater with on-site temperature feedback control. *Micromachines* **9**, 170 (2018).
34. Bae, S. et al. Roll-to-roll production of 30-inch graphene films for transparent electrodes. *Nat. Nanotechnol.* **5**, 574–578 (2010).
35. DiMarco, J. P. & Philbrick, J. T. Use of ambulatory electrocardiographic (Holter) monitoring. *Ann. Intern. Med.* **113**, 53–68 (1990).
36. Montain, S. J. & Ely, M. *Water Requirements and Soldier Hydration* (Borden Institute). https://ke.army.mil/bordeninstitute/other_pub/hydrationpdf.pdf
37. Sawka, M. N., Cheuvront, S. N. & Kenefick, R. W. High skin temperature and hypohydration impair aerobic performance. *Exp. Physiol.* **97**, 327–332 (2012).
38. Kumari, P., Mathew, L. & Syal, P. Increasing trend of wearables and multimodal interface for human activity monitoring: a review. *Biosens. Bioelectron.* **90**, 298–307 (2017).
39. Barea Navarro, R., Boquete Vázquez, L. & López Guillén, E. EOG-based wheelchair control. in *Smart Wheelchairs and Brain-Computer Interfaces* 381–403 (Elsevier, 2018). https://doi.org/10.1016/B978-0-12-812892-3.00016-9
40. Sel, K., Ibrahim, B. & Jafari, R. ImpediBands: body coupled bio-impedance patches for physiological sensing proof of concept. *IEEE Trans. Biomed. Circuits Syst.* **14**, 757–774 (2020).
41. Ibrahim, B. & Jafari, R. A novel method for continuous blood pressure monitoring using wrist-worn bio-impedance sensors. *2018 IEEE Biomed. Circuits Syst. Conf. BioCAS 2018 - Proc.* 3–6 (2018). https://doi.org/10.1109/BIOCAS.2018.8584783
42. Masvidal-Codina, E. et al. High-resolution mapping of infraslow cortical brain activity enabled by graphene microtransistors. *Nat. Mater.* **18**, 280–288 (2019).
43. Polat, E. O. et al. Flexible graphene photodetectors for wearable fitness monitoring. *Sci. Adv.* **5**, eaaw7846 (2019).
44. Miao, P. et al. Graphene nanostructure-based tactile sensors for electronic skin applications. *Nano-Micro Lett* **11**, 71 (2019).
45. Saccomandi, P. et al. Microfabricated tactile sensors for biomedical applications: a review. *Biosensors* **4**, 422–448 (2014).
46. Chortos, A., Liu, J. & Bao, Z. Pursuing prosthetic electronic skin. *Nat. Mater.* **15**, 937–950 (2016).
47. Chang, T. H., Li, K., Yang, H. & Chen, P. Y. Multifunctionality and mechanical actuation of 2D materials for skin-mimicking capabilities. *Adv. Mater.* **30**, 1–13 (2018).
48. Akinwande, D., Petrone, N. & Hone, J. Two-dimensional flexible nanoelectronics. *Nat. Commun.* **5**, 5678 (2014).
49. Qiao, Y. et al. Graphene-based wearable sensors. *Nanoscale* **11**, 18923–18945 (2019).
50. Amjadi, M., Kyung, K.-U., Park, I. & Sitti, M. Stretchable, skin-mountable, and wearable strain sensors and their potential applications: a review. *Adv. Funct. Mater.* **26**, 1678–1698 (2016).
51. Jang, H., Dai, Z., Ha, K.-H., Ameri, S. K. & Lu, N. Stretchability of PMMA-supported CVD graphene and of its electrical contacts. *2D Mater* **7**, 014003 (2019).
52. Yetisen, A. K., Martinez-Hurtado, J. L., Ünal, B., Khademhosseini, A. & Butt, H. Wearables in medicine. *Adv. Mater.* **30**, e1706910 (2018).
53. Tricoli, A., Nasiri, N. & De, S. Wearable and miniaturized sensor technologies for personalized and preventive medicine. *Adv. Funct. Mater.* **27**, 1–19 (2017).
54. Griss, P., Tolvanen-Laakso, H. K., Meriläinen, P. & Stemme, G. Characterization of micromachined spiked biopotential electrodes. *IEEE Trans. Biomed. Eng.* **49**, 597–604 (2002).
55. Kirkup, L. & Searle, A. A direct comparison of wet, dry and insulating bioelectric recording electrodes. *Physiol. Meas.* **21**, 271 (2000).
56. Giffney, T., Bejanin, E., Kurian, A. S., Travas-Sejdic, J. & Aw, K. Highly stretchable printed strain sensors using multi-walled carbon nanotube/silicone rubber composites. *Sensors Actuators A Phys* **259**, 44–49 (2017).
57. Cheng, Y., Wang, R., Zhai, H. & Sun, J. Stretchable electronic skin based on silver nanowire composite fiber electrodes for sensing pressure, proximity, and multidirectional strain. *Nanoscale* **9**, 3834–3842 (2017).
58. Herbert, R., Kim, J. H., Kim, Y. S., Lee, H. M. & Yeo, W. H. Soft material-enabled, flexible hybrid electronics for medicine, healthcare, and human-machine interfaces. *Materials (Basel)* **11**, 187 (2018).
59. Kang, J., Tok, J. B. H. & Bao, Z. Self-healing soft electronics. *Nat. Electron.* **2**, 144–150 (2019).
60. Bauer, S. et al. 25th anniversary article: A soft future: From robots and sensor skin to energy harvesters. *Adv. Mater.* **26**, 149–162 (2014).
61. Pang, C., Lee, C. & Suh, K. Y. Recent advances in flexible sensors for wearable and implantable devices. *J. Appl. Polym. Sci.* **130**, 1429–1441 (2013).
62. Nezakati, T., Seifalian, A., Tan, A. & Seifalian, A. M. Conductive polymers: opportunities and challenges in biomedical applications. *Chem. Rev.* **118**, 6766–6843 (2018).
63. Bihar, E. et al. Fully printed all-polymer tattoo/textile electronics for electromyography. *Flex. Print. Electron.* **3**, 034004 (2018).
64. Ferrari, L. M. et al. Ultraconformable temporary tattoo electrodes for electrophysiology. *Adv. Sci.* **5**, 1700771 (2018).

65. Yeo, W. H. et al. Multifunctional epidermal electronics printed directly onto the skin. *Adv. Mater.* **25**, 2773–2778 (2013).
66. Huang, X., Yeo, W. H., Liu, Y. & Rogers, J. A. Epidermal differential impedance sensor for conformal skin hydration monitoring. *Biointerphases* **7**, 1–9 (2012).
67. Gutruf, P. & Rogers, J. A. Implantable, wireless device platforms for neuroscience research. *Curr. Opin. Neurobiol.* **50**, 42–49 (2018).
68. Ferrari, L. M., Ismailov, U., Badier, J.-M., Greco, F. & Ismailova, E. Conducting polymer tattoo electrodes in clinical electro- and magneto-encephalography. *npj Flex. Electron.* **4**, 1–9 (2020).
69. Webb, R. C. et al. Ultrathin conformal devices for precise and continuous thermal characterization of human skin. *Nat. Mater.* **12**, 938–944 (2013).
70. Bariya, M., Nyein, H. Y. Y. & Javey, A. Wearable sweat sensors. *Nat. Electron.* **1**, 160–171 (2018).
71. Chung, H. J. et al. Stretchable, multiplexed pH sensors with demonstrations on rabbit and human hearts undergoing ischemia. *Adv. Healthc. Mater.* **3**, 59–68 (2014).
72. Miyamoto, A. et al. Inflammation-free, gas-permeable, lightweight, stretchable on-skin electronics with nanomeshes. *Nat. Nanotechnol.* **12**, 907–913 (2017).
73. Gong, S. et al. Local crack-programmed gold nanowire electronic skin tattoos for in-plane multisensor integration. *Adv. Mater.* **31**, 1–8 (2019).
74. Ershad, F. et al. Ultra-conformal drawn-on-skin electronics for multifunctional motion artifact-free sensing and point-of-care treatment. *Nat. Commun.* **11**, 3823 (2020).
75. Pan, C. et al. Visually imperceptible liquid-metal circuits for transparent, stretchable electronics with direct laser writing. *Adv. Mater.* **30**, 1706937 (2018).
76. Childres, I., Jauregui, L. A., Tian, J. & Chen, Y. P. Effect of oxygen plasma etching on graphene studied using Raman spectroscopy and electronic transport measurements. *New J. Phys.* **13**, 025008 (2011).
77. Liu, N. et al. Ultratransparent and stretchable graphene electrodes. *Sci. Adv.* **3**, e1700159 (2017).

Acknowledgements

This work was supported in part by the Office of Naval Research grant N00014-18-1-2706. We also acknowledge the support, in part, of National Science Foundation (NSF) grant 2031674. We thank F. Qing of UESTC, and NASCENT-Grolltex collaboration for providing us with large-scale CVD-grown graphene.

Author contributions

S.K.A., N.L. and D.A. conceived the idea and performed initial experiments. D.K. and S.K.A. optimized the procedure. D.K. and S.K.A. developed the protocol. D.K., S.K.A., A.N., H.J. and J.K. performed the experiments and analyzed the data. D.K. complied the data, wrote the manuscript, and designed the video supplements. All authors discussed the results and contributed to the editing of the manuscript.

Competing interests

The authors declare no competing interests.

Additional information

Supplementary information The online version contains supplementary material available at https://doi.org/10.1038/s41596-020-00489-8.

Correspondence and requests for materials should be addressed to D.K.

Peer review information *Nature Protocols* thanks Mario Caironi, Wenlong Cheng and the other, anonymous, reviewer(s) for their contribution to the peer review of this work.

Reprints and permissions information is available at www.nature.com/reprints.

Publisher's note Springer Nature remains neutral with regard to jurisdictional claims in published maps and institutional affiliations.

Received: 26 August 2020; Accepted: 17 December 2020;
Published online: 12 April 2021

Related links
Key references using this protocol:
Kabiri Ameri, S. et al. *ACS Nano* **11**, 7634–7641 (2017): https://doi.org/10.1021/acsnano.7b02182
Ameri, S. K. et al. *npj 2D Mater. Appl.* **2**, 1–7 (2018): https://doi.org/10.1038/s41699-018-0064-4
Sel, K. et al. *BioCAS 2019 - Biomed. Circuits Syst. Conf. Proc.* 1–4 (2019): https://doi.org/10.1109/BIOCAS.2019.8919003

nature research

Corresponding author(s): Dmitry Kireev

Last updated by author(s): Oct 6, 2020

Reporting Summary

Nature Research wishes to improve the reproducibility of the work that we publish. This form provides structure for consistency and transparency in reporting. For further information on Nature Research policies, see our Editorial Policies and the Editorial Policy Checklist.

Statistics

For all statistical analyses, confirm that the following items are present in the figure legend, table legend, main text, or Methods section.

n/a	Confirmed	
☐	☒	The exact sample size (*n*) for each experimental group/condition, given as a discrete number and unit of measurement
☐	☒	A statement on whether measurements were taken from distinct samples or whether the same sample was measured repeatedly
☒	☐	The statistical test(s) used AND whether they are one- or two-sided *Only common tests should be described solely by name; describe more complex techniques in the Methods section.*
☒	☐	A description of all covariates tested
☒	☐	A description of any assumptions or corrections, such as tests of normality and adjustment for multiple comparisons
☒	☐	A full description of the statistical parameters including central tendency (e.g. means) or other basic estimates (e.g. regression coefficient) AND variation (e.g. standard deviation) or associated estimates of uncertainty (e.g. confidence intervals)
☒	☐	For null hypothesis testing, the test statistic (e.g. *F*, *t*, *r*) with confidence intervals, effect sizes, degrees of freedom and *P* value noted *Give P values as exact values whenever suitable.*
☒	☐	For Bayesian analysis, information on the choice of priors and Markov chain Monte Carlo settings
☒	☐	For hierarchical and complex designs, identification of the appropriate level for tests and full reporting of outcomes
☒	☐	Estimates of effect sizes (e.g. Cohen's *d*, Pearson's *r*), indicating how they were calculated

Our web collection on statistics for biologists contains articles on many of the points above.

Software and code

Policy information about availability of computer code

Data collection	Hioki LCR Sample Application, Hioki HiTESTER, OpenBCI GUI, Keysight GUI Data Logger Software For Handheld LCR Meter
Data analysis	MS Excel, Origin Pro

For manuscripts utilizing custom algorithms or software that are central to the research but not yet described in published literature, software must be made available to editors and reviewers. We strongly encourage code deposition in a community repository (e.g. GitHub). See the Nature Research guidelines for submitting code & software for further information.

Data

Policy information about availability of data

All manuscripts must include a data availability statement. This statement should provide the following information, where applicable:

- Accession codes, unique identifiers, or web links for publicly available datasets
- A list of figures that have associated raw data
- A description of any restrictions on data availability

The data supporting the findings of this study are available within the paper and its supplementary source data files.

Field-specific reporting

Please select the one below that is the best fit for your research. If you are not sure, read the appropriate sections before making your selection.

☒ Life sciences ☐ Behavioural & social sciences ☐ Ecological, evolutionary & environmental sciences

For a reference copy of the document with all sections, see nature.com/documents/nr-reporting-summary-flat.pdf

Life sciences study design

All studies must disclose on these points even when the disclosure is negative.

Sample size	During impedance measurements, at least three tattoos of each kind were were used as a single set, recording three pairs: 1-2, 1-3, and 2-3. Each time the sweep was performed three times with 10 sec interval.
Data exclusions	No data was excluded from the analysis.
Replication	Two sets of each graphene type (multuple GETs per type) were used for the study
Randomization	Not applicable.
Blinding	Not applicable.

Reporting for specific materials, systems and methods

We require information from authors about some types of materials, experimental systems and methods used in many studies. Here, indicate whether each material, system or method listed is relevant to your study. If you are not sure if a list item applies to your research, read the appropriate section before selecting a response.

Materials & experimental systems

n/a	Involved in the study
☒	☐ Antibodies
☒	☐ Eukaryotic cell lines
☒	☐ Palaeontology and archaeology
☒	☐ Animals and other organisms
☐	☒ Human research participants
☒	☐ Clinical data
☒	☐ Dual use research of concern

Methods

n/a	Involved in the study
☒	☐ ChIP-seq
☒	☐ Flow cytometry
☒	☐ MRI-based neuroimaging

Human research participants

Policy information about studies involving human research participants

Population characteristics	*Describe the covariate-relevant population characteristics of the human research participants (e.g. age, gender, genotypic information, past and current diagnosis and treatment categories). If you filled out the behavioural & social sciences study design questions and have nothing to add here, write "See above."*
Recruitment	All of the measurements were performed on the manuscript authors by themselves.
Ethics oversight	UT Austin IRB #2018-06-0058

Note that full information on the approval of the study protocol must also be provided in the manuscript.